1964

Control system for shipboard landing of VTOL type aircraft

Easterling, Crawford Alan.; Fieser, Arnold Kerp.

Massachusetts Institute of Technology

T-395

CONTROL SYSTEM FOR SHIPBOARD LANDING OF VTOL TYPE AIRCRAFT

by

Crawford Alan Easterling
Arnold Kerp Fieser

September 1964

Degrees Of
Engineer In Aeronautics And Astronautics
Master Of Science

CONTROL SYSTEM FOR SHIPBOARD LANDING OF VTOL TYPE AIRCRAFT

by

CRAWFORD ALAN EASTERLING
LIEUTENANT COMMANDER, USN
BEE, Rensselaer Polytechnic Institute
(1951)

ARNOLD KERP FIESER
LIEUTENANT, USN
BSME, University of Illinois
(1954)

SUBMITTED IN PARTIAL FULFILLMENT
OF THE REQUIREMENTS FOR THE
DEGREES OF ENGINEER IN AERONAUTICS AND ASTRONAUTICS
AND MASTER OF SCIENCE
at the
MASSACHUSETTS INSTITUTE OF TECHNOLOGY
September 1964

CONTROL SYSTEM FOR SHIPBOARD LANDING OF VTOL TYPE AIRCRAFT

by

Crawford A. Easterling
Arnold K. Fieser

Submitted to the Department of Aeronautics and Astronautics, Massachusetts Institute of Technology, in August 1964, in partial fulfillment of the requirements for the degrees of Engineer in Aeronautics and Astronautics and Master of Science.

ABSTRACT

The design of a control system to land VTOL aircarft on ships underway is considered. The effect of ship dynamics on the control of the landing aircraft is investigated. A destroyer is taken as a representative ship, and the placement of the landing platform to minimize the effects of ship motion is determined. Positioning of the aircraft for landing is accomplished by tracking the line of sight vector from the aircraft to thelanding platform and commanding the velocity of the aircraft with signals proportional to coordinate angles of the vector. Analog simulation is used extensively in the investigation. It is determined that such a system is feasable and that the rate of descent of the aircraft can be commanded independently of the motions of the ship.

Thesis Supervisor: H. P. Whitaker
Title: Associate Professor of Aeronautics and Astronautics

ACKNOWLEDGMENTS

The authors wish to express their appreciation to Professor H. P. Whitaker for his assistance as thesis advisor.

Acknowledgment is made of the advice given by Dr. S. Waldron and Mr. R.A. MacDonald of the Institute of Naval Studies.

Thanks go to Mr. Ralph Trueblood and to Dr. W. Bryant of the M.I.T. Instrumentation Laboratory for their encouragement during the writing of this thesis.

Finally, our thanks go to Carol Mitcham and Margaret Keith for typing the manuscript.

The Helicopter flight control system assumed for the studies of this thesis is an adaptation of a system developed by the MIT Instrumentation Laboratory under DSR Project 54-190, sponsored by the U.S. Army Transportation Research Command under Contract DA-44-177-TC-757.

TABLE OF CONTENTS

LIST OF ILLUSTRATIONS

LIST OF SYMBOLS AND TERMS

X_f, Y_f, Z_f	Axes of the f frame. (Coordinate frames are defined in Appendix B).
I	Inertial Coordinate Frame.
E	Earth Centered Coordinate Frame.
L	Earth Local Vertical Frame.
A	Aircraft Body Coordinate Frame.
EA	Earth Aircraft Coordinate Frame.
AM	Air Mass Coordinate Frame.
H	Heading - the angle of rotation about the Z_L axis from X_L to X_{EA}.
E	Elevation - the angle of rotation about the Y_{EA} axis from the X_{EA} to X_A. In linearized equations, this same notation indicates the perturbation quantity,
θ	Pitch - the angle of rotation about the Y_A axis from the X_{EA}-Y_{EA} plane to X_A.
ϕ	Roll - the angle of rotation about the X_A axis from Y_{EA} to Y_A.
W	Angular velocity.
V	Linear velocity.
a	Linear acceleration.
$W_{(r-f)_*}$	Component about the * axis of the angular velocity of frame f with respect to the reference frame, r.
$V_{(r-f)_*}$	Component parallel to the * axis of the linear velocity of frame f with respect to the reference frame r.

$a_{(r-f)_*}$	Component parallel to the * axis of the linear acceleration of frame f with respect to the reference frame, r.
W_*	A perturbation angular velocity which is indicative of $W_{(r-f)_*}$ minus any initial steady state value.
V_*	A perturbation linear velocity which is indicative of $V_{(r-f)_*}$ minus any initial steady state value .
mg	Gross weight.
Ix	Moment of inertia about the X_A axis.
Iy	Moment of inertia about the Y_A axis.
Iz	Moment of inertia about the Z_A axis.
I_{xz}	Cross-product of inertia about the X_A and Z_A axis.
IW	Angular momentum of the aircraft.
$\bar{F}$	A force vector.
F_x	Component of force parallel to the X_A axis.
F_y	Component of force parallel to the Y_A axis.
F_z	Component of force parallel to the Z_A axis.
$\bar{M}$	A moment vector.
L	Component of moment about the X_A axis.
M	Component of moment about the Y_A axis.
N	Component of moment about the Z_A axis.
$X_{( )}$	Dimensional force coefficient due to ( ); used in compiling F_x.
$Y_{( )}$	Dimensional force coefficient due to ( ); used in compiling F_y.
$Z_{( )}$	Dimensional force coefficient due to ( ); used in compiling F_z.

$L_{(\,)}$	Dimensional moment coefficient due to ( ); used in compiling L.
$M_{(\,)}$	Dimensional moment coefficient due to ( ); used in compiling M.
$N_{(\,)}$	Dimensional moment coefficient due to ( ); used in compiling N.

Subscripts for coefficients

p	Angular velocity of the aircraft about the X_A axis with respect to the air mass.
q	Angular velocity of the aircraft about the Y_A axis with respect to the air mass.
r	Angular velocity of the aircraft about the Z_A axis with respect to the air mass.

Control displacements are used also as subscripts for coefficients

δe	Control displacement controlling the moment about the Y_A axis.
δa	Control displacement controlling the moment about the X_A axis.
δr	Control displacement controlling the moment about the Z_A axis.
δz	Control displacement controlling the force parallel to the Z_A axis.
p	The LaPlace operator.
τ	A time constant
$PFol_{m \to n}$	An open loop performance function from m to n.
$PFcl_{m \to n}$	A closed loop performance function from m to n.
VTOL	Vertical take off and landing.

IVMS — Inertial velocity measurement system of the velocity flight control system.

Symbols used to describe ship motion

$\underline{x}$ — distance measured along the longitudinal axis of the ship from the center of gravity; measured positive forward.

$\underline{z}_{cg}$ — vertical displacement of the center of gravity of a ship from an equilibrium position.

$\underline{z}$ — vertical displacement of a particular deck station.

ψ — pitch angle of a ship.

ϵ — phase angle between pitch and heave of a ship.

ω — pitch and heave response frequency of a ship to a sinusoidal wave forcing function.

Symbols introduced for the vector angle command system

$\overline{LOS}$ — The line of sight is the vector from the aircraft to the point of intended landing.

$\bar{R}$ — A vector of unit length the direction of which is defined by the $\overline{LOS}$.

R_* — The component of $\bar{R}$ parallel to the * axis.

x — The component of the $\overline{LOS}$ parallel to the X_{EA} axis.

y — The component of the $\overline{LOS}$ parallel to the Y_{EA} axis.

h — The component of the $\overline{LOS}$ parallel to the Z_{EA} axis. This is the altitude of the aircraft above the point of intended landing.

α_f — Control angle measured in the $X_f Z_f$ plane from the Z_f axis to the projection of $\overline{LOS}$ in the $X_f Z_f$ plane.

β_f — Control angle measured in the plane formed by the $\overline{LOS}$ and the Y_f axis from the projection of LOS in the $X_f Z_f$ plane to $\overline{LOS}$.

The conventional dot notation ($\dot{X}$, $\dot{V}$, etc.) is employed to indicate the time derivative of a quantity.

A barred quantity ($\bar{V}$, $\bar{F}$, etc.) indicates a vector quantity with both magnitude and direction.

A subscript of o on a quantity ($V_{X_{Ao}}$, $V_{Y_{Ao}}$, etc.) indicates an initial condition.

A subscript of $_c$ on a quantity ($V_{X_{A_c}}$, h_c, etc.) indicates a commanded quantity.

Any further subscripting is self explanatory.

CHAPTER I

INTRODUCTION

The feasability of operating aircraft from the deck of a ship was demonstrated forty-four years ago and became a reality when the USS Langley was commissioned in 1922. For many years after the first aircraft was landed aboard ship, the pilot had the job of effecting a safe landing with the help of but a few crude instruments. With the advent of radar, electronic navigation aids, and much improved instruments to assist in making approaches to a landing under adverse weather conditions, it was still the pilot who had to make the final landing virtually unassisted. Today the pilot is aided by an optical "glide slope" in effecting precision landings of conventional aircraft aboard aircraft carriers and fully automatic systems have been demonstrated.

The helicopter ushered in the age of vertical take off and landing (VTOL) aircraft and present military operations indicate that these aircraft are becoming of increasing importance. The application of VTOL aircraft in Naval operations was immediate. Today, the anti-submarine helicopter, the vertical assualt aircraft, and logistic helicopters are extensively operated from ships at sea. In the high performance aircraft of today, the thrust is rapidly approaching the weight of the aircraft. Therefore the development of a VTOL "strike" aircraft is imminent.

The desirability of operating such aircract from any size fighting ship is clear, however problems in landing on a small ship are multiplied by the more severe motions of the ship and much smaller landing platform. This dictates that precision landings must be attained. To effectively operate VTOL aircraft from these ships, a landing system is required to accurately position and land the aircraft in any weather or sea conditions where operations would be feasable.

The methods of landing on small ships that are presently used are all primarily pilot controlled. This requires the pilot to be in visual contact with the landing platform and to have enough other visual clues to allow him to control the aircraft near hover flight. There are two known operational methods of making the actual landing. One method is to wait until a quiescent period occurs in the motion of the ship and then to land as quickly as possible. The other method is that of hauling the hovering aircraft down to the deck using a cable attached to the under side of the aircraft and a constant torque winch mounted on the ship's deck. This is sometimes termed the "winch down" method.

Both of these methods have the undesirable feature of requiring sufficient visibility to find the landing platform and to control the aircraft. Even in clear weather, the visual clues for control would be marginal if not unacceptable at night. An undesirable feature in the second method is the requirement for connecting a cable from an airborn helicopter to a moving ship. The tension on the cable in the second method also tends to make the automatically stabalized helicopter tend toward instability. Admittedly, this method should not be discarded since there are a great number of unstable helicopters being flown by pilots today.

The purpose of this study is to investigate the feasability of a flight control system which would accurately position and land a VTOL aircraft on a small ship. In this study, a preliminary design of a control system which will perform this function is presented. Due to the complexity of the problem, a detailed analog simulation of a VTOL aircraft including six degrees of freedom was used extensively.

CHAPTER II

LANDING SYSTEM REQUIREMENTS

It is apparent that if flight operations are to be conducted in all weather conditions and around the clock, a landing system is required that will eliminate or at least minimize the visual clue requirement of the pilot. Examining the present procedures used by the U.S. Navy in night hovering of anti-submarine helicopters, the pilot's duties become those of commanding and monitoring the flight control system. As the first specification for the landing control system, requirements of the pilot should be reduced to attaining an acceptable approach position, introducing the initial command inputs, and thereafter monitoring the operation of the system.

A VTOL aircraft, at hover or near hover velocities, is inherently unstable. It is presumed that a means of automatically stabilizing the basic aircraft is available and this requirement is not placed upon the landing control system.

Several aircraft navigation systems used in the fleet today are capable of positioning the aircraft on a desired radial from the ship at 1/2 nautical mile. The landing system should be capable of controlling the aircraft from the 1/2 mile circle to a safe landing aboard ship.

The landing system should not be expected to perform under meteorological conditions in which the aircraft would not operate. For purposes of this study, a limit of 40 knots is placed upon wind velocity. This constitutes a galeforce wind.

The fact that the landing area is on the deck of a ship underway poses several unique problems. Some reasonable bounds must be placed upon ship motion to permit the conduct of flight operations. These bounds, as well as ship motion in general, must be investigated. It must be recognized, however, that even though the control engineer cannot regulate the motion of the ship, the control system he designs must be capable of effecting a safe landing despite the motion of the ship. This motion places several requirements upon the landing system. The relative aircraft vertical velocity with respect to the deck at the time of touchdown must be limited by structural considerations. Present military specifications[2] for VTOL aircraft limit this velocity to 8 fps. The relative attitude of the aircraft with respect to the deck at the time of touchdown must be controlled to prevent excessive stress in the landing gear. The relative position of the aircraft with respect to the desired landing point on the deck must be controlled to within defined limits at the time of landing. The final problem associated with ship motion is that of securing the aircraft after contact has been made with the deck. Several methods are used by various navies today to overcome this problem. They include attaching a cable from a deck winch to the aircraft during the final phases of the approach and increasing cable tension when the aircraft touches the deck. Other methods[3] include suction cups on the aircraft undercarriage or driving an harpoon from the aircraft into a flexible deck grating on touchdown. The problem of securing the aircraft after landing is not a part of this investigation.

Because of the high rates of fuel consumption of VTOL aircraft in or near hover flight, the approach and landing should be made as expeditiously as possible. Fig. 1 shows the rates of fuel consumption for present and anticipated types of VTOL aircraft[4] while hovering.

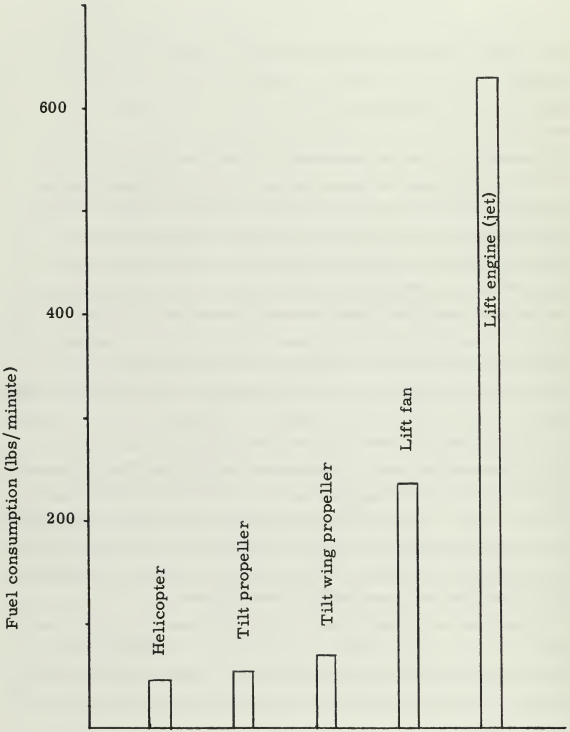

Fig. 1 Fuel consumption of VTOL aircraft in hovering flight (G. W. 35,000 lbs)

Associated with most VTOL aircraft, there is a power failure curve which shows, in the event of engine failure, the combinations of altitude and air speed that will permit a controlled landing. Fig. 2 is representative of these curves. Since present VTOL aircraft are not equipped with pilot escape devices, pilot safety would dictate that the minimum possible time be spent in the "unsafe" region of the power failure curve during the approach to a landing.

The landing system should be versatile enough to be used ashore in various operating conditions, such as crude landing fields in forward combat areas, and still be as simple as possible.

Finally, it is desirable that minimum changes in the course and speed of the ship be required to recover aircraft. These requirements constitute a brief description of the problem and are the guidelines within which this investigation is conducted.

The motions of ships 400 and 600 feet long are investigated in Chapter III. These ship lengths embrace destroyers and are considered to be representative of small ships from which VTOL aircraft might operate. The hull shape and length of a destroyer, then, define the ship model of this investigation.

The MIT Velocity Flight Control System is described in Appendix C, and block diagrams of the system are shown in Figs. C-1 and C-2. It is used here to stabilize the basic aircraft and to generate an aircraft velocity in response to a command input. It is for the landing system under investigation to develop the necessary command inputs.

The Vertol 107-M(CH-46) helicopter was chosen as the model VTOL aircraft since this helicopter was used as the "test bed" for flight testing the Velocity Flight Control System and the system gains were available for this aircraft.

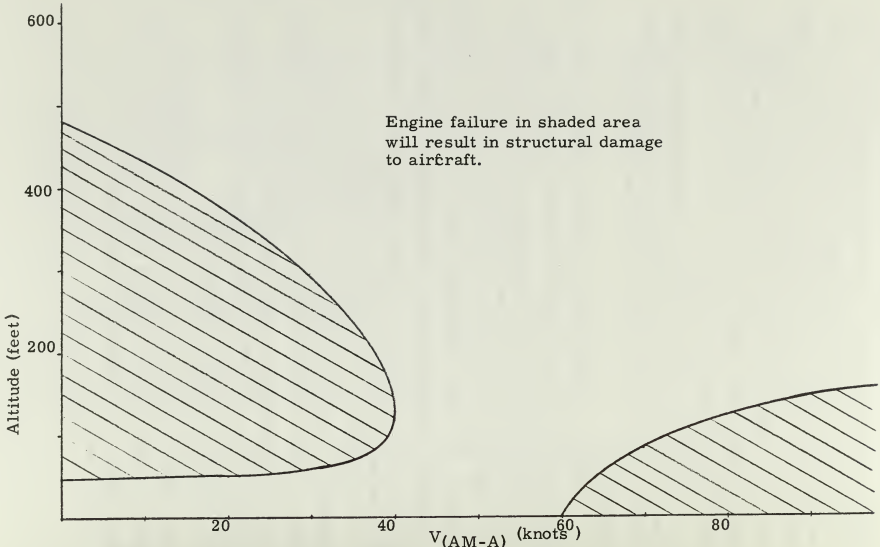

Fig. 2 Altitude limits for safe landing after power failure (typical helicopter)

CHAPTER III

THE INFLUENCE OF SHIP MOTION ON VTOL OPERATIONS

The motions of a ship underway at sea are caused by the transfer of energy from the waves on the ocean surface to the ship. A ship has six degrees of freedom in which to respond to the excitations of the waves. Consider a coordinate frame comprised of a longitudinal, a lateral, and a vertical axis fixed in the ship with the origin at the ship's center of gravity. Surge, sway, and heave are defined as translations along the three respective axes. Roll, pitch, and yaw are the angular displacements about the three respective axes. These instantaneous translations and displacements are superimposed upon the steady state translation of the ship. Sway, surge, and yaw contribute little to the total motion of the ship and no consideration will be given to their effect. Roll is the major factor in lateral motion while pitch and heave account for the vertical motion. Coupling between the lateral and vertical motions is small and the two can be considered separately.

The motions of a ship are difficult, if not impossible, to predict over any appreciable time period by any but statistical methods. By sensing acceleration, impending ship motions may be anticipated for short time intervals only. Both methods of determining ship motion are used in this investigation.

Roll is the least amenable to analysis and very little information is available in the literature on this subject. Roll can be minimized by heading the ship into the wave train.[5] A more desirable method is to stabilize the ship in roll be mechanical means. Tests conducted on the USS Compass Island

indicate that the roll of a ship can be reduced by a factor of 5 using roll stabilization. The lateral movement of the ship caused by roll complicates the problem of positioning the aircraft for landing. The roll angle influences the relative attitude between the aircraft and the ship at the time of landing. Roll is simulated in this study by sinusoids of 1/2 and 1 radian per second since the natural frequency of a destroyer in roll is within this frequency range. (3)

The pitch and heave of a ship are more periodic in nature than is roll and therefore more susceptable to analysis. They are of prime concern here since they directly influence the relative vertical velocity of the aircraft with respect to the deck at the time of landing. Ref. 6 was prepared as a guide for aircraft designers seeking to estimate structural and controllability requirements associated with vertical landings on moving ships. A procedure is developed in the reference for determining the statistical probability of vertical deck displacement due to pitch and heave. A summary of the method is given in Appendix A. This method is used here to calculate the probability of deck vertical velocity and is based upon emperical wave data taken in the North Atlantic. The emperical data is based upon observations taken by weather ships over an extended period of time and all subsequent investigation of vertical deck motion makes use of these observations.

Gale force winds (40 knots) have been defined as the maximum in which landings will be attempted. Winds in excess of 40 knots occur 2.2% of all time in the North Atlantic. Therefore 97.8% of all time is defined as "usable time". Some reasonable bounds must also be placed upon ship motion for the operation of VTOL aircraft. "Slamming" of a ship occurs when the forefoot of the bow lifts out of the water and subsequently reenters resulting in high stresses within the ship. For this reason, slamming is a practical limit for the operation of a

ship as dictated by good seamanship. Vertical deck motions associated with a ship at the verge of slamming are taken to be the limiting case for aircraft operations.

Since a limit is imposed upon the relative vertical velocity of the aircraft with respect to the deck,[2] some knowledge of the deck vertical velocity is necessary. The method summarized in Appendix A was used to determine the probability of occurrence of a particular vertical velocity as a function of deck station. The response frequency of a ship to a wave forcing function is the same in pitch as in heave. Heave displacement lags pitch by an emperically determined phase angle of 60 degrees. Using the probability of heave rate and pitch rate given in Appendix A, the probability of vertical velocity was computed with the following equations:

$$\dot{\underline{z}} = \dot{\underline{z}}_{cg} \sin(\omega t - \epsilon) + \underline{x}\,\dot{\psi} \sin \omega t \qquad (3\text{-}1)$$

$$\dot{\underline{z}} = (\dot{\underline{z}}_{cg} \cos E + \underline{x}\dot{\psi}) \sin \omega t - \dot{\underline{z}}_{cg} \sin \omega t \cos \omega t \qquad (3\text{-}2)$$

$$\dot{\underline{z}} = [\dot{z}^2_{cg} + 2\,\underline{x}\dot{\psi}\,\dot{\underline{z}}_{cg} \cos \omega t + \underline{x}^2 \dot{\psi}^2]^{\frac{1}{2}} \qquad (3\text{-}3)$$

The probability of vertical velocity is plotted vs deck station in Figs. 3, 4, 5, and 6 for ships 400 and 600 feet long steaming into the waves at 10 and 20 knots. Figs. 7, 8, 9, and 10 present the same information plotted as the percent of usable time that a particular vertical velocity will not be exceeded at a given deck station. It is to be remembered that these curves represent the motion of a ship on the verge of slamming in the North Atlantic.

It can be seen that the deck station which experiences the minimum vertical motion is 1/2 to 2/3 of the ship length aft of the bow. From the standpoint of ship motion, this relatively tranquil deck station is the desired landing area.

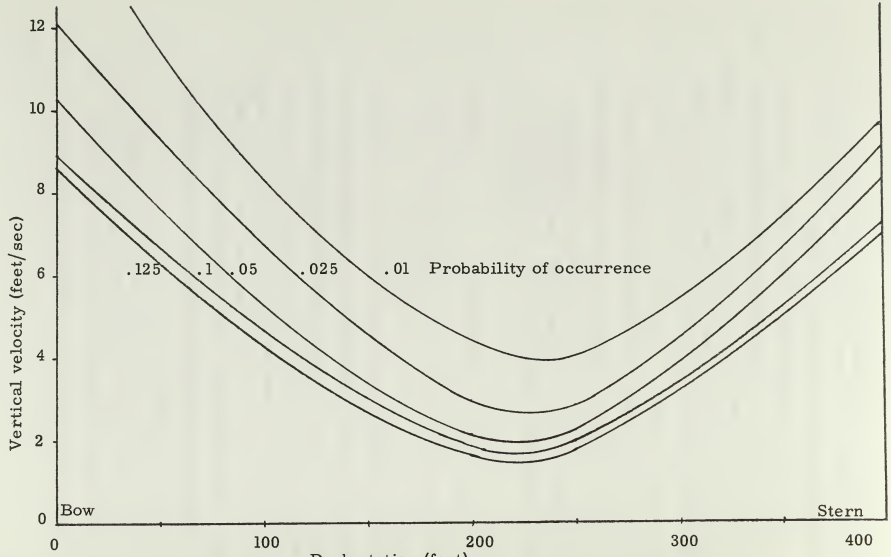

Fig. 3 Vertical velocity vs position of landing area - probability of occurrence
400 ft ship into waves at 10 knots

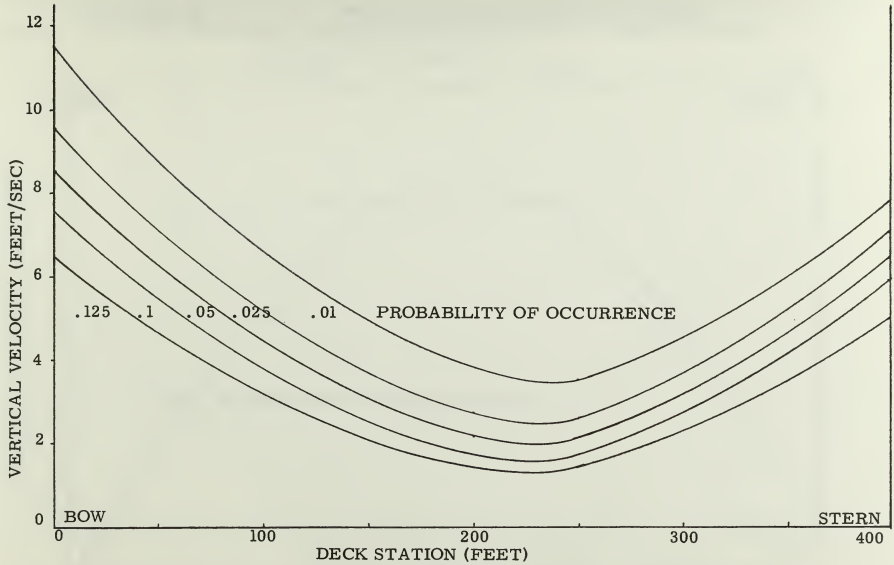

FIG. 4 VERTICAL VELOCITY VS POSITION OF LANDING AREA - PROBABILITY OF OCCURENCE 400 FT SHIP INTO WAVES AT 20 KNOTS

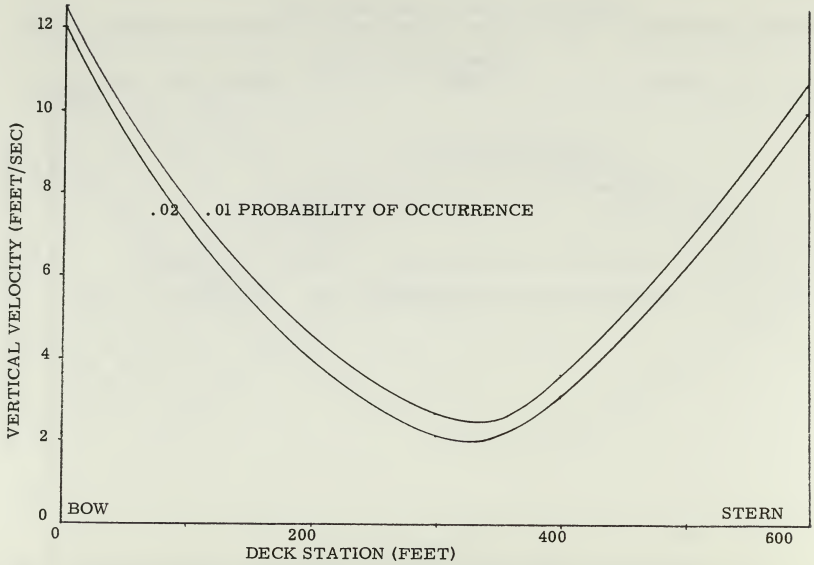

FIG. 5 VERTICAL VELOCITY VS POSITION OF LANDING AREA - PROBABILITY OF OCCURRENCE 600 FT SHIP INTO WAVES AT 10 KNOTS

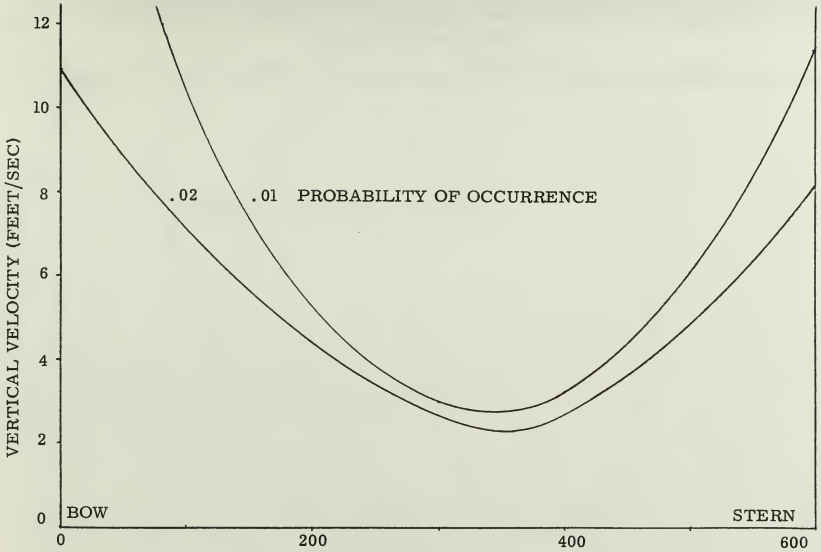

FIG. 6 VERTICAL VELOCITY VS POSITION OF LANDING AREA - PROBABILITY OF OCCURRENCE 600 FT SHIP INTO WAVES AT 20 KNOTS

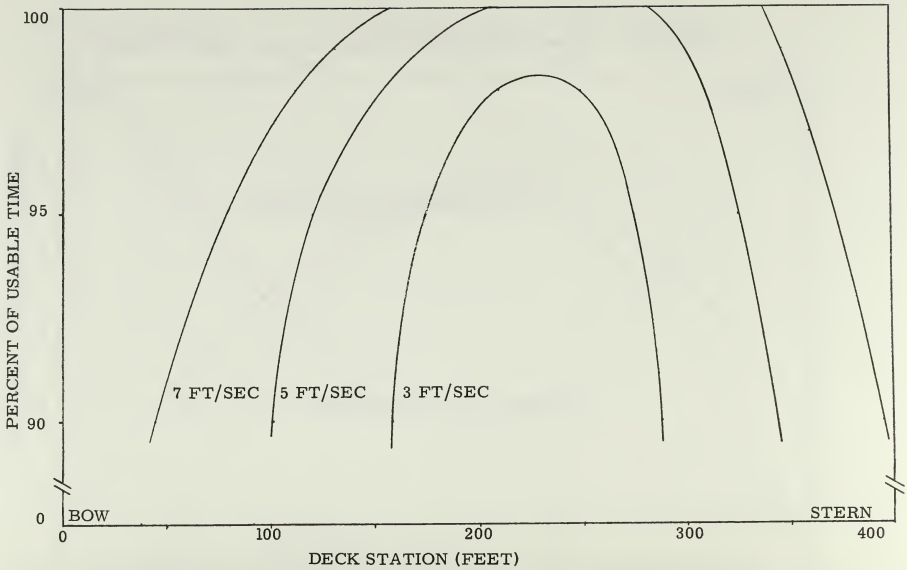

FIG. 7 USABLE DECK VS VERTICAL VELOCITY - 400 FT SHIP INTO WAVES AT 10 KNOTS

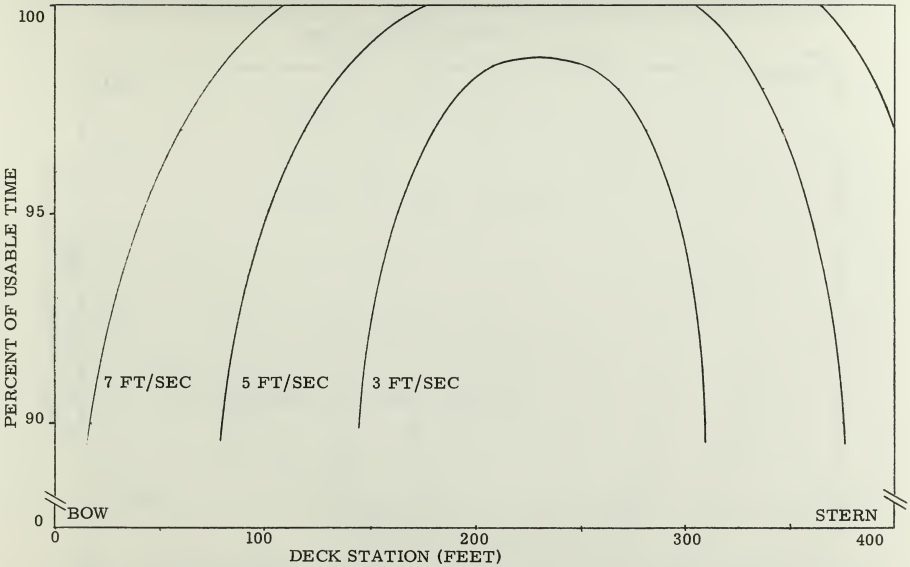

FIG. 8 USABLE DECK VS VERTICAL VELOCITY - 400 FT SHIP INTO WAVES AT 20 KNOTS

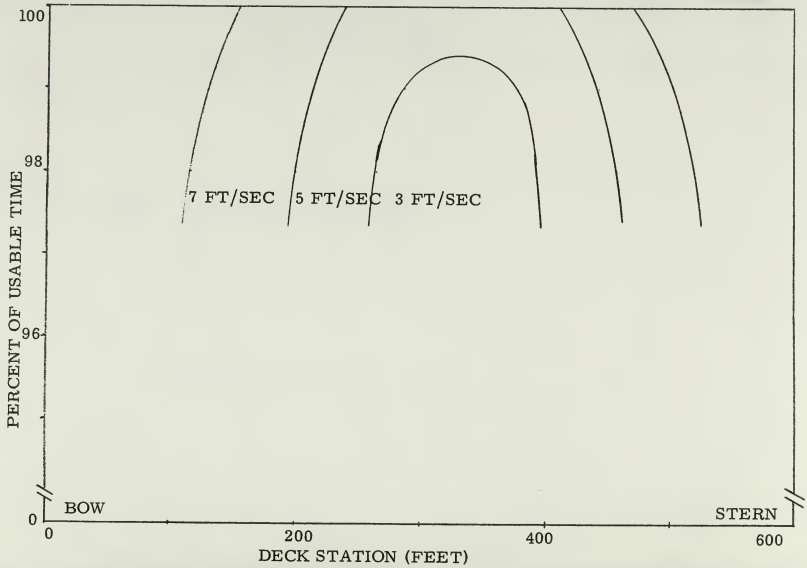

FIG. 9 USABLE DECK VS VERTICAL VELOCITY - 600 FT SHIP INTO WAVES AT 10 KNOTS

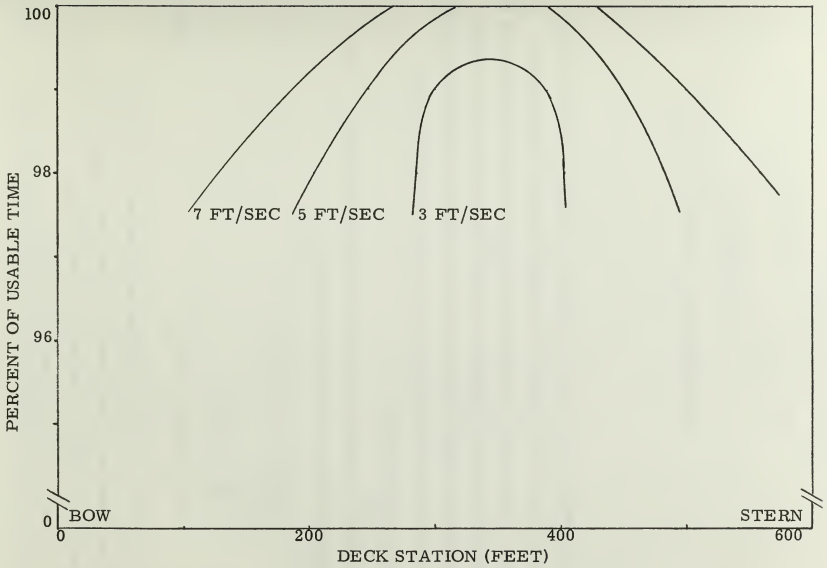

FIG. 10 USABLE DECK VS VERTICAL VELOCITY - 600 FT SHIP INTO WAVES AT 20 KNOTS

CHAPTER IV

THE VECTOR ANGLE COMMAND SYSTEM

The Vector Angle Command System incorporates a sensor to track the direction of the vector from the aircraft to the intended point of landing. This sensor is instrumented so as to measure two angles in the aircraft body frame. These angles form the basis of command signals to the Velocity Flight Control System to position the aircraft for landing. This method of vector tracking provides position feedback for the Velocity Control System.

The vector angles in the body frame are shown in Fig. 11. The components of $\bar{R}$ in the A frame are defined by

$$R_{X_A} = \cos \alpha_A \cos \beta_A$$

$$R_{Y_A} = \sin \beta_A$$

$$R_{Z_A} = \sin \alpha_A \cos \beta_A \qquad (4-1)$$

The components of $\bar{R}$ in the EA frame are obtained by use of the following coordinate transformation. The Euler angles used are generated in the IVMS of the Velocity Control System. The coordinate transformation is shown below in matrix form.

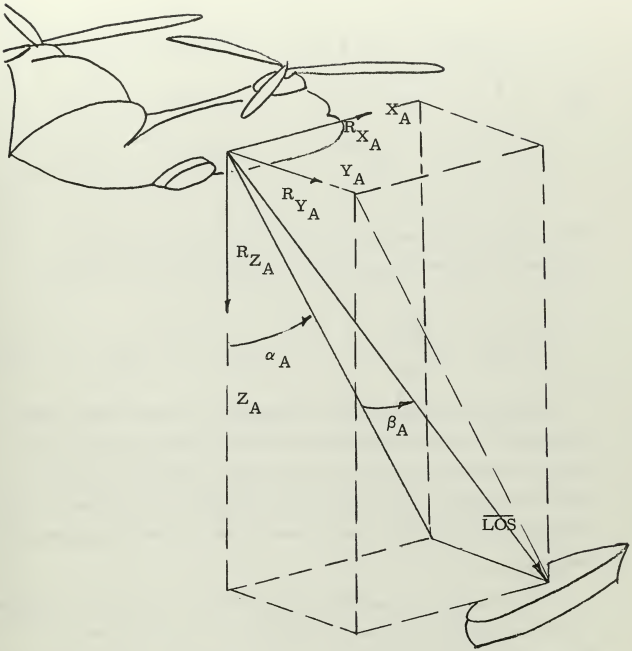

FIG. 11 LINE OF SIGHT VECTOR IN AIRCRAFT BODY COORDINATES

$$\bar{R}_{EA} = \begin{bmatrix} \cos E & \sin E \sin \phi & \sin E \cos \phi \\ 0 & \cos \phi & -\sin \phi \\ -\sin E & \cos E \sin \phi & \cos E \cos \phi \end{bmatrix} \begin{bmatrix} R_{X_A} \\ R_{Y_A} \\ R_{Z_A} \end{bmatrix} \tag{4-2}$$

The components of the unit vector in the EA frame are used to compute tan α_{EA} and β_{EA} of Fig. 12 by the following relations.

$$\tan \alpha_{EA} = \frac{R_{X_{EA}}}{R_{Z_{EA}}} \qquad \beta_{EA} = \sin^{-1} R_{Y_{EA}} \tag{4-3}$$

Altitude is available to an accuracy of $\pm$5 percent from a radar altimeter[7]. An inertial-barometer altitude sensing system in the Velocity Flight Control System also provides altitude information. Prior knowledge of the height of the landing area is presumed. Altitude is subsequently taken to mean above the landing platform of the ship.

To develop the Vector Angle Control System, the aircraft equations of motion in Appendix B are linearized about an air mass velocity ($\bar{V}_{(AM-A)}$) of 40 knots. The trimmed flight condition, about which the equations are linearized, is described by

$V_{(E-A)_{X_{Ao}}} = 68$ fps $\qquad \phi_o = 0$

$V_{(E-A)_{Y_{Ao}}} = 0 \qquad E_o = 7^o$

$V_{(E-A)_{Z_{Ao}}} = 8.3$ fps

θ is approximated by E. The assumptions associated with small

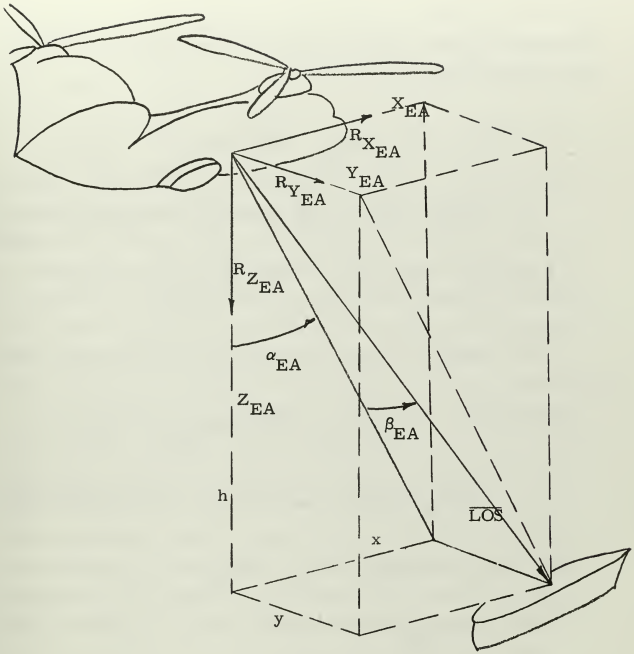

FIG. 12 LINE OF SIGHT VECTOR IN EARTH-AIRCRAFT COORDINATES

perturbations about a trimmed condition are described in Appendix B. The linearized equations of motion are

$$F_x = m\left[\dot{V}_{X_A} + W_{Y_A} V_{(I-A)_{Z_{Ao}}} - W_{Z_A} V_{(I-A)_{Y_{Ao}}}\right] = X_{V_X} V_{X_A}$$

$$+ X_q W_{Y_A} + X_{V_Z} V_{Z_A} + X_{\delta e}\delta e + X_{\delta z}\delta z - (mg \cos E_o)\,\Delta E \tag{4-4}$$

$$F_y = m\left[\dot{V}_{Y_A} + W_{Z_A} V_{(I-A)_{X_{Ao}}} - W_{X_A} V_{(I-A)_{Z_{Ao}}}\right] = Y_p W_{X_A}$$

$$+ Y_r W_{Z_A} + Y_{V_Y} V_{Y_A} + Y_{\delta r}\delta r + Y_{\delta a}\delta a + (mg \cos E_o)\,\phi \tag{4-5}$$

$$F_z = m\left[\dot{V}_{Z_A} + W_{X_A} V_{(I-A)_{Y_{Ao}}} - W_{Y_A} V_{(I-A)_{X_{Ao}}}\right] = Z_{V_X} V_{X_A}$$

$$+ Z_q W_{Y_A} + Z_{V_Z} V_{Z_A} + Z_{\delta e}\delta e + Z_{\delta z}\delta z - (mg \sin E_o)\,\Delta E \tag{4-6}$$

$$L = I_x \dot{W}_{X_A} - I_{xz} \dot{W}_{Z_A} = L_p W_{X_A} + L_r W_{Z_A}$$

$$+ L_{V_Y} V_{Y_A} + L_{\delta r}\delta r + L_{\delta a}\delta a \tag{4-7}$$

$$M = I_y \dot{W}_{Y_A} = M_{V_X} V_{X_A} + M_q W_{Y_A} + M_{V_Z} V_{Z_A}$$

$$+ M_{\delta e}\delta e + M_{\delta z}\delta z \tag{4-8}$$

$$N = I_z \dot{W}_{Z_A} - I_{xz} \dot{W}_{X_A} = N_p W_{X_A} + N_r W_{Z_A}$$

$$+ N_{V_Y} V_{Y_A} + N_{\delta r}\delta r + N_{\delta a}\delta a \tag{4-9}$$

The force and moment coefficients are contained in Tables B-I and B-II. These equations and the Velocity Control System were simulated on an analog computer. Details of the simulation are included as Appendix D.

FLIGHT PROFILE

Heading The flight profile of the landing approach is influenced by the requirements defined in Chapter II. The roll of a ship can be minimized by heading the ship into the waves[5]. Since the wind and the waves will generally come from the same direction[5], heading the ship into the waves will result in a small angle between the reciprocal of the relative wind vector and the course of the ship. The approach course of the aircraft is on a line of constant bearing from the ship (radial) and into the relative wind. The approach is made by commanding a constant heading parallel to the approach course. This heading is a required input to the system prior to the approach. V_{Y_A} is commanded independent of the aircraft heading, but once on the desired inbound radial, the approach is made in coordinated flight since no trim roll angle is required to track the ship. Finally, most proposed VTOL aircraft have tricycle landing gear. The nose gear is designed to withstanding much less loading than the main landing gear. Since the amplitude of pitch of the ship (Fig. A-2) is less than that of roll[3], the pitch attitude of the aircraft, relative to the deck, can be more easily controlled if the angle between the aircraft heading and the course of the ship is small. An angle of 10 degrees between the headings of the ship and of the aircraft is taken as representative. This also keeps the turbulence caused by the superstructure of the ship clear of the approach track.

Altitude A commanded approach altitude of fifty feet is considered the minimum consistent with safety. No obstructions to flight, except the ship, exist in an over-water approach. This altitude has the

advantage of permitting the entire approach and landing to be made on the "safe" side of the power failure curve. The pilot retains the option of commanding any approach altitude, however 50 ft is used for design considerations since it is most demanding of the system. The approach altitude is maintained until the aircraft is over the deck of the ship with no relative velocity. This permits the pilot to monitor the system and command the final descent.

The final descent is made vertically. This precludes tracking the vertical motions of the ship and the predominant random motions, which then require tracking, are those caused by roll. The vertical velocity of the deck of a ship 400 feet long just aft of amidship does not exceed 5 fps under the conditions stipulated (Figs. 7 and 8). No attempt is made to anticipate the vertical motion of the ship. The vertical velocity of the aircraft is programmed as a function of altitude. The aircraft descends at 8.3 fps until the desired approach altitude is reached. Once the final descent is commanded, the aircraft descends at 5 fps to an altitude of 20 feet at which time a transition to 2 fps is initiated. This insures that the relative vertical velocity will not exceed 8 fps when the landing is made. These rates of descent are expeditious yet consistent with safety and standard all-weather operating procedures[8].

Velocity $A\,V_{(E-A)_{X_{Ao}}}$ of 40 knots is commanded to close the ship from the 1/2 mile arc. This approach velocity is consistent with present operating procedure. Since $\bar{V}_{(E-AM)}$ was limited to 40 knots in Chapter III, the range of $\bar{V}_{(AM-A)}$ becomes 0 to 80 knots.

The pilot positions the aircraft for the landing approach as shown in Fig. 13.

Guidance of the aircraft is assumed by the Landing System upon command of the pilot after the vector has been established by the sensor and no later than the 1/2 mile arc. Desired approach altitude,

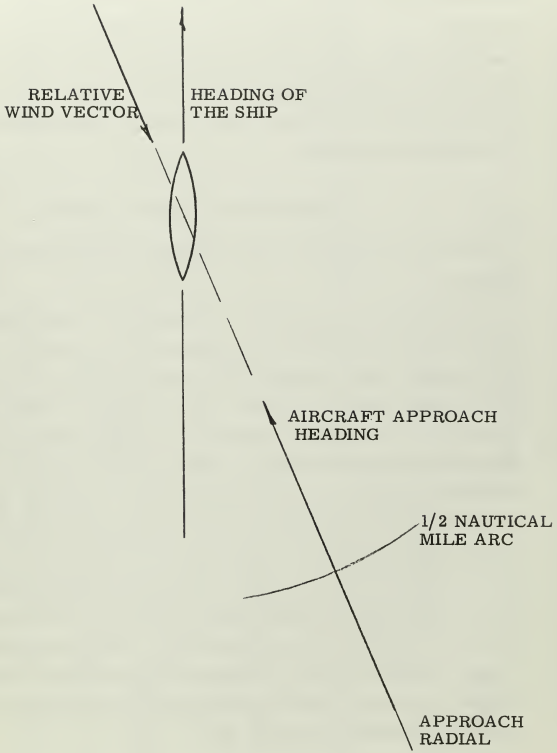

FIG. 13 THE APPROACH RADIAL

height of the landing deck above sea level, and approach heading are required pilot inputs. The heading is held constant during the approach. V_{X_A} is commanded by tan α_{EA} to close the ship. V_{Y_A} is commanded by β_{EA} to hold the aircraft on the inbound radial. $\dot{h}$ is programmed as a function of altitude and position. The longitudinal and lateral command channels function independently and are considered separately.

LONGITUDINAL COMMAND CHANNEL

Fig. 14 is a functional block diagram of the longitudinal command channel.

Fig. 15 shows V_{X_C} vs x for a ship speed of 0 knots and an approach altitude of 50 feet. V_{X_C} generated by α_{EA} and by tan α_{EA} are compared. With the angle as the command signal, deceleration from 40 knots begins at 1/2 mile. Using the tangent of the angle to command, deceleration is delayed until 400 feet from the ship. Analog simulation showed that an overshoot of the ship could not be prevented using α_{EA} as the command signal. By making V_{X_C} proportional to tan α_{EA} a smooth transition from 40 knots to the velocity of the ship could be accomplished by delaying the transition until 400 feet from the ship. By making the system gain a linear function of the commanded approach altitude, this transition was made uniform for any approach altitude. Lead-lag compensation is used to improve the system response in the transition to the velocity of the ship. For zero ship speed, V_{X_A} and $\dot{x}$ have the same value and the desired $\dot{x}$ is linear with x.

For any ship speed other than zero, the rate of closure is decreased and a steady state error in x is required to track the ship. Since the desired $\dot{x}$ for a ship speed of zero is a linear function of x, a comparison with the actual $\dot{x}$ could provide a command signal to

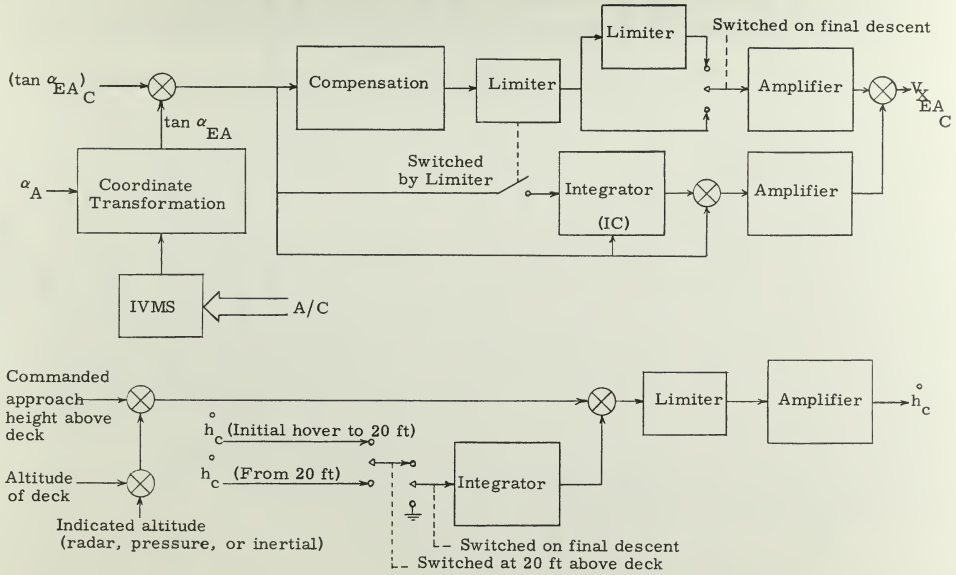

FIG. 14 FUNCTIONAL BLOCK DIAGRAM OF THE LONGITUDINAL COMMAND SYSTEM

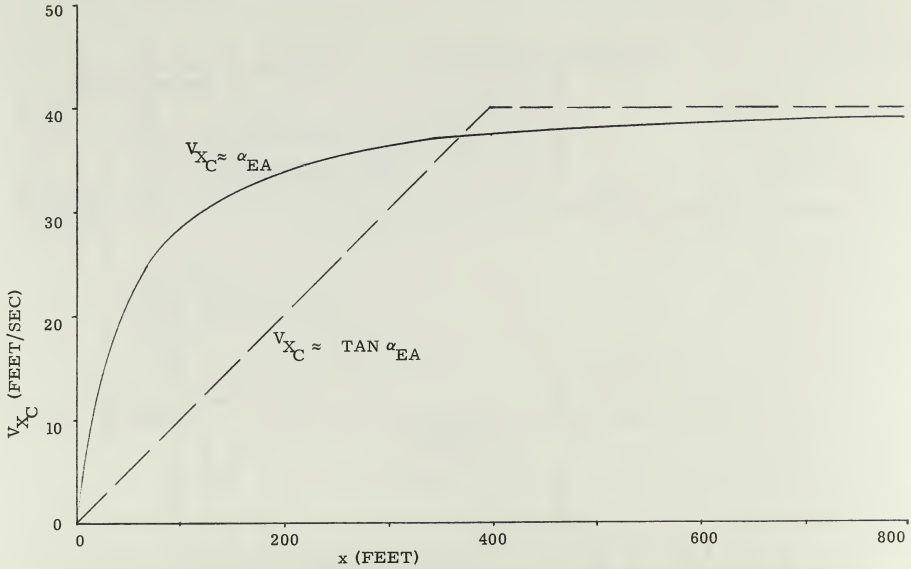

FIG. 15 COMMANDED APPROACH VELOCITY VS DISTANCE FROM THE LANDING PLATFORM

improve the closure rate. By integrating this signal, the steady state error could also be eliminated. Fig. 16 shows how this signal might be generated. Since $\dot{x}$ is not readily available, Fig. 17 shows the same signal generated without $\dot{x}$ as an input. x_o is the distance from the ship at time t_o when deceleration of the aircraft is initiated. By either method, V_{X_C} is the same and is expressed by Eq. 4-10.

$$V_{X_C} = C_3 \int_{t_o}^{t} C_1 x \, dt + x - x_o + C_2 x \qquad (4\text{-}10)$$

Equation 4-10 is helpful in explaining how the signal of the vernier circuit is shaped. It does not define the final command signal.

Fig. 14 also shows the functional block diagram for generating $\dot{h}_c$. Altitude is obtained from the radar altimeter during the approach and from the inertial barometric system when over the ship.

Final descent over the ship is commanded by the pilot. The commanded vertical velocity is changed from 5 fps to 2 fps by a comparator when h is 20 feet.

Fig. 18 is a mathematical block diagram of the entire longitudinal control system. Certain linearizing assumptions are made to investigate the stability of the system in the final descent. Tan α_{EA} is approximated by α_{EA}. The Velocity Control System is assumed linear and x is obtained by integrating V_{X_A}. Eqs. 4-11, 4-12, and 4-13 are the aircraft longitudinal equations of motion linearized about the trim condition at 40 knots.

$$(p+.0454)\, V_{X_A} + (8.28\, p + 32.2)E + .0104\, V_{Z_A} = 9.44\, \delta z \qquad (4\text{-}11)$$

$$.278\, V_{X_A} - (63.7p)\, E + (p + .628)\, V_{Z_A} = 423.\, \delta z \qquad (4\text{-}12)$$

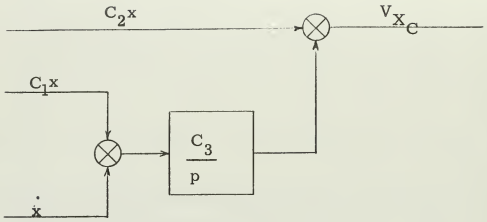

C_1, C_2, AND C_3 ARE CONSTANTS; $x \approx h_c \text{ TAN } \alpha_{EA}$

FIG. 16 BLOCK DIAGRAM OF $V_{X_{A_c}}$ VERNIER USING $\dot{x}$.

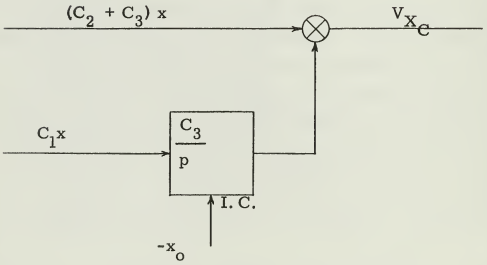

C_1, C_2, AND C_3 ARE CONSTANTS; $x \approx h_c \text{ TAN } \alpha_{EA}$

FIG. 17 BLOCK DIAGRAM OF $V_{X_{A_c}}$ VERNIER USING x.

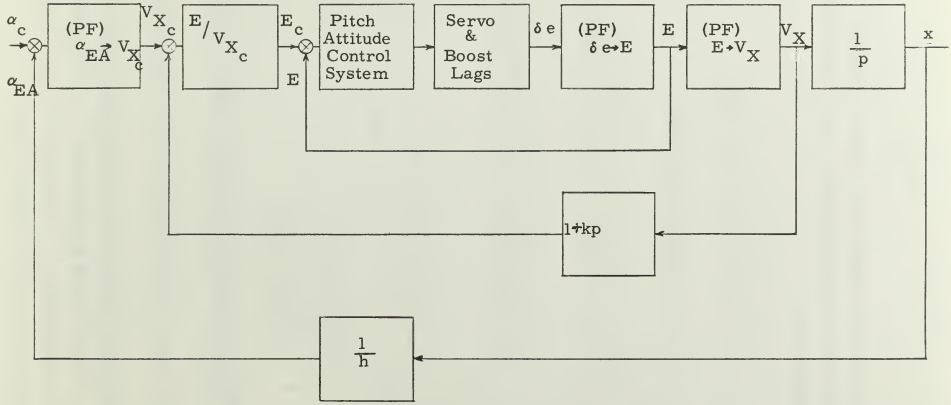

FIG. 18 MATHEMATICAL BLOCK DIAGRAM OF THE LONGITUDINAL CONTROL CHANNEL

$$.0155V_{X_A} + (p^2 + 1.94p)\,E - .0241V_{Z_A} = .433\,\delta e + 3.76\,\delta z \qquad (4\text{-}13)$$

The aircraft transfer functions are derived from these equations. The collective is assumed fixed and δz is zero. Aircraft pitch angle is approximated by E.

$$(PF)_{\delta e \rightarrow E} = \frac{.433(p+.686)\,(p+.018)}{(p-.705)(p+2.673)(p+.323 \pm j.426)} \qquad (4\text{-}14)$$

$$(PF)_{E \rightarrow V_X} = \frac{.995(p-10.0)\,(p+3.33)\,(p+.606)}{(p+.686)\,(p+.018)} \qquad (4\text{-}15)$$

$$(PF)cl_{E_c \rightarrow E} = \frac{7812.(p+.686)(p+.018)(p+1.405)(p+.285)}{(p+.053 \pm j.038)(p+.748 \pm j.673)(p+2.79 \pm j3.91)(p+18.64 \pm j5.66)} \qquad (4\text{-}16)$$

$$(PF)cl_{V_{X_c} \rightarrow V_X} = \frac{-187.26(p+1.405)(p+.285)(p-10.0)(p+3.33)(p+.606)}{(p+7.55)(p+29.46)(p+.255 \pm j.160)(p+.925 \pm j.763)(p+2.54 \pm j6.87)} \qquad (4\text{-}17)$$

$$(PF)ol_{\alpha_{EA_c} \rightarrow V_{X_c}} = \frac{2.1\,h_c\,(p+.087)(p+.353)}{p(p+3)} \qquad (4\text{-}18)$$

$$(PF)cl_{\alpha_{EA_c} \rightarrow X} = \frac{h_c\,393.2\,C}{D + \frac{h_c}{h}\,393.2C} \qquad (4\text{-}19)$$

$C = \ldots (p+.087)(p+.285)(p+.353)(p+.606)(p+.141)(p+3.33)(p-10.0)$

$D = p^2(p+3.00)(p+7.55)(p+29.46)(p+.255 \pm j.160)(p+.925 \pm .763)(p+2.54 \pm j6.87)$

Equation 4-19 is the closed loop performance function of the system with the aircraft hovering over the ship. Fig. 19 is a root locus plot with decreasing altitude. It can be seen that the system becomes unstable between 5 and 6 feet above the deck.

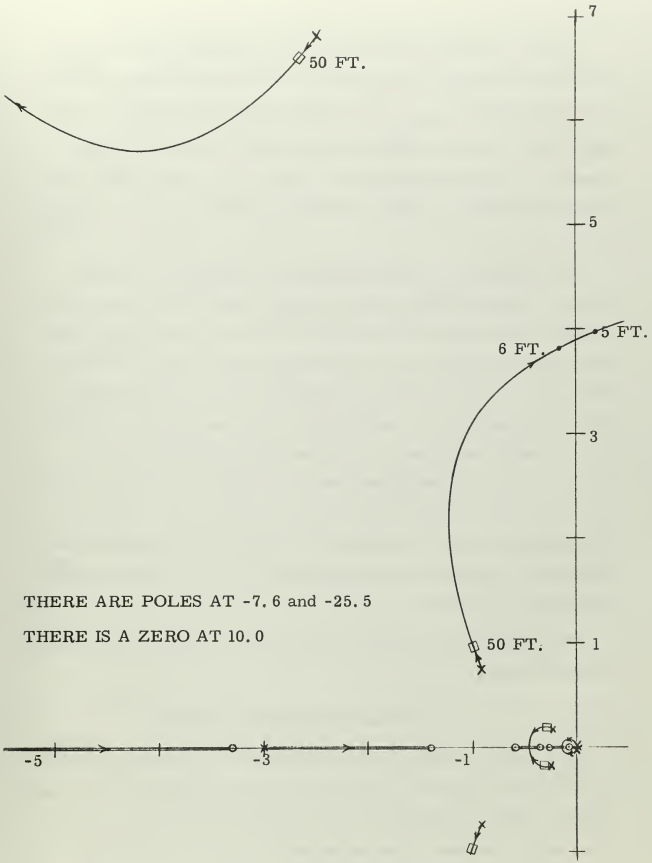

FIG. 19 LOCUS OF THE ROOTS OF (PF) cl WITH DECREASING $\alpha_{EA \rightarrow x}$ ALTITUDE.

Figs. A-2 and A-3 show that the pitch angle of the ship will not exceed 4 degrees. Since the trim pitch angle of the aircraft is 7 degrees when $V_{(AM-A)_{X_A}}$ is 40 knots, the possibility of a "nose gear first" landing is eliminated by limiting E to plus or minus 2 degrees. This is accomplished by limiting V_{X_C}, as shown in Fig. 14, when the aircraft is over the ship and the final descent to a landing is begun.

This limit on V_{X_C} also stabilized the longitudinal command channel. With this limit on the command signal, the system is still capable of tracking the ship at all ship speeds investigated. This analysis is confirmed by the results of analog simulation shown in Figs. 20, 21, and 22. These recordings show the transition to ship velocities of 0, 10, and 20 knots. The descent is terminated at h = 2 feet in each case to show the stabilizing effect of the limiter. Fig. 21 shows the response to a surge in ship motion which was simulated by an impulse in x at h = 30 feet. Fig. 23 shows the surge response of the system at h = 2 feet. For all ship speeds simulated, the landing was accomplished within 90 seconds after passing the 1/2 mile arc.

Wind gusts have negligible effect upon the ability of the system to track the ship.

LATERAL COMMAND CHANNEL

The lateral command channel provides the command signals in V_{Y_A} to hold the aircraft on the desired radial during the approach and landing. Since the headings of the aircraft and the ship differ by a small angle, tracking of the lateral excursions of the deck due to roll of the ship is controlled by this channel. The functional block diagram of the channel is shown in Fig. 24 and the mathematical block diagram in Fig. 25. The angle β_{EA}, rather than the tangent

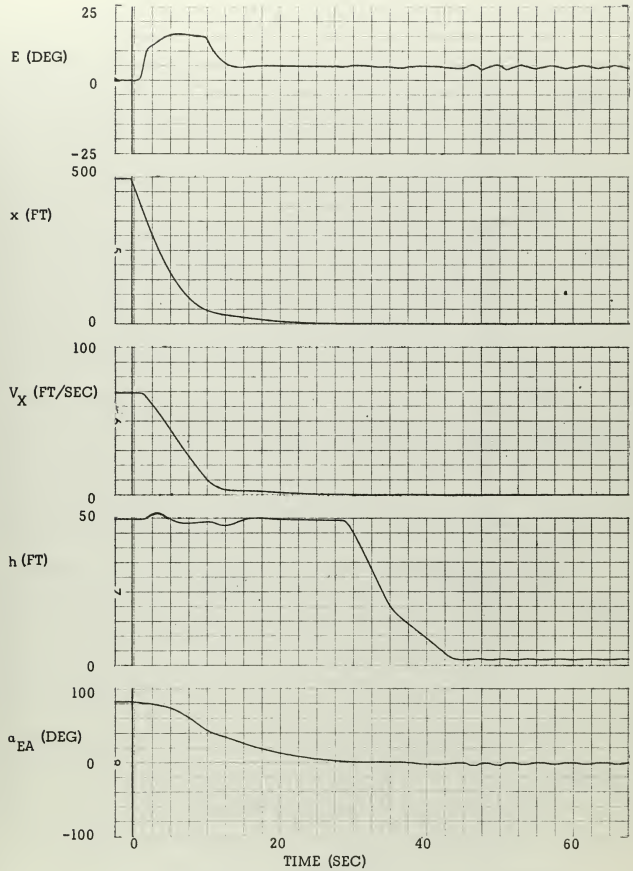

FIG. 20 RESPONSE OF THE LONGITUDINAL SYSTEM - AIRCRAFT DECELERATING TO A SHIP SPEED OF 0 KNOTS.

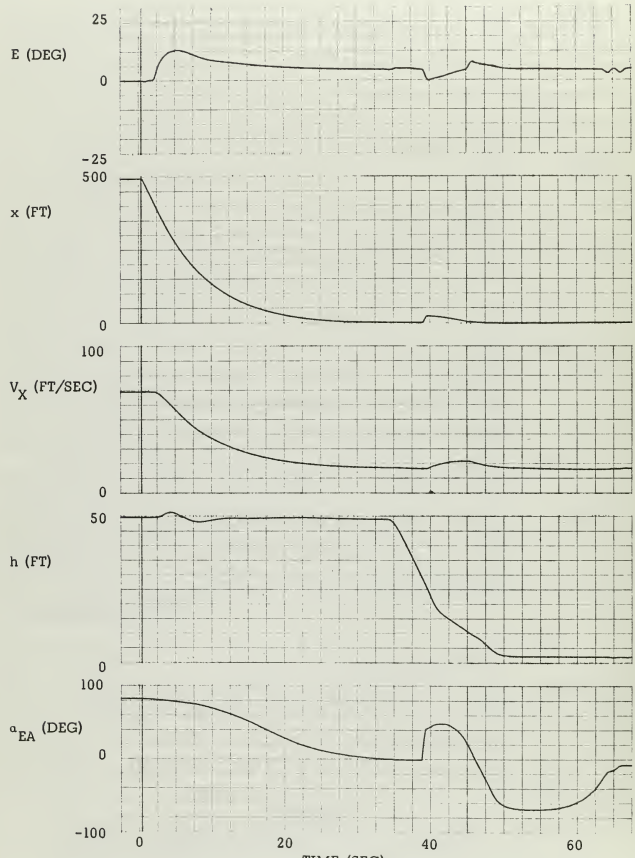

FIG. 21 RESPONSE OF THE LONGITUDINAL SYSTEM - AIRCRAFT DECELERATING TO A SHIP SPEED OF 10 KNOTS - PERTURBATION IN x AT h = 30 FEET.

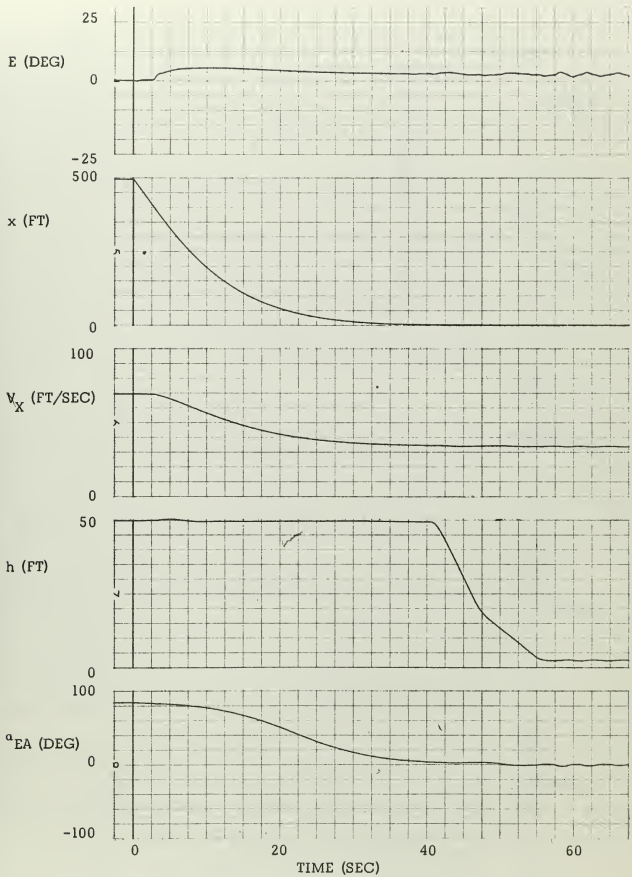

FIG. 22 RESPONSE OF THE LONGITUDINAL SYSTEM - AIRCRAFT DECELERATING TO A SHIP SPEED OF 20 KNOTS.

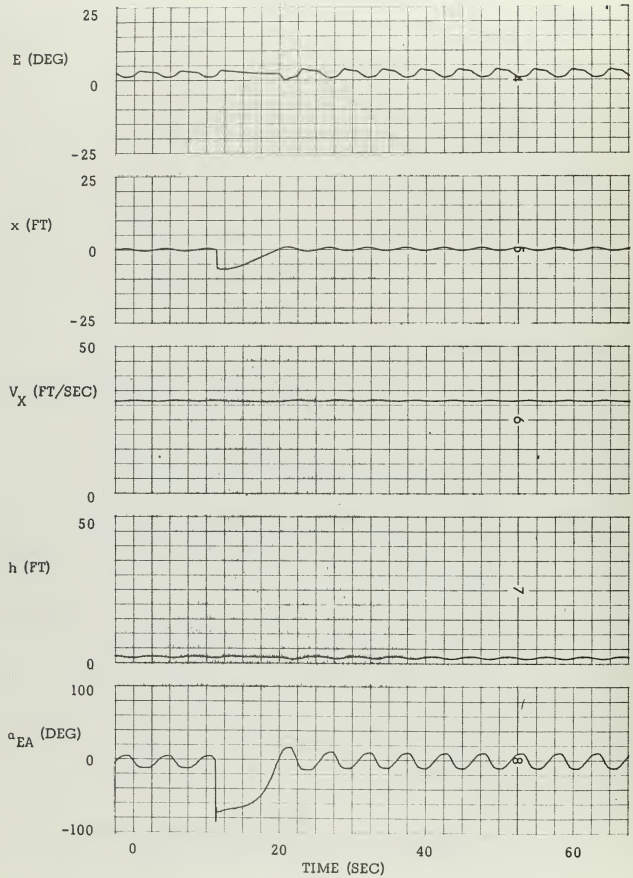

FIG. 23 RESPONSE OF THE LONGITUDINAL SYSTEM TO A PERTURBATION IN x AT h = 2 FEET.

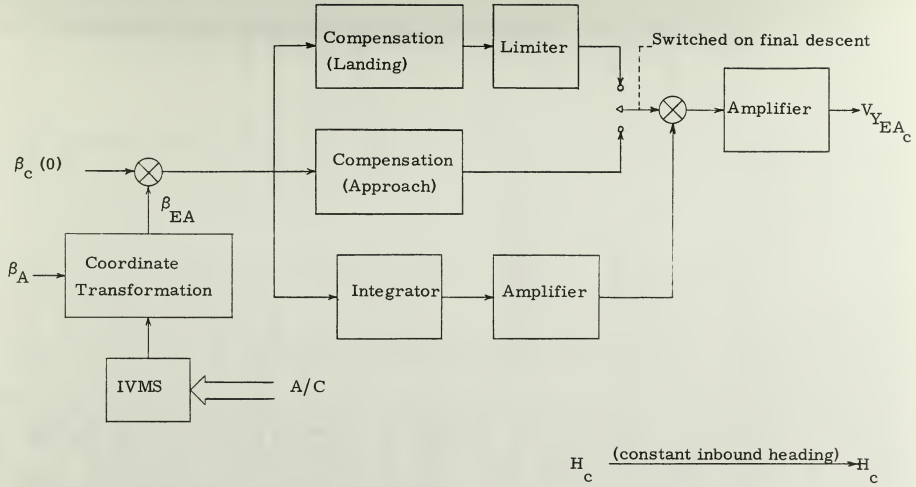

FIG. 24 FUNCTIONAL BLOCK DIAGRAM OF THE LATERAL COMMAND CHANNEL

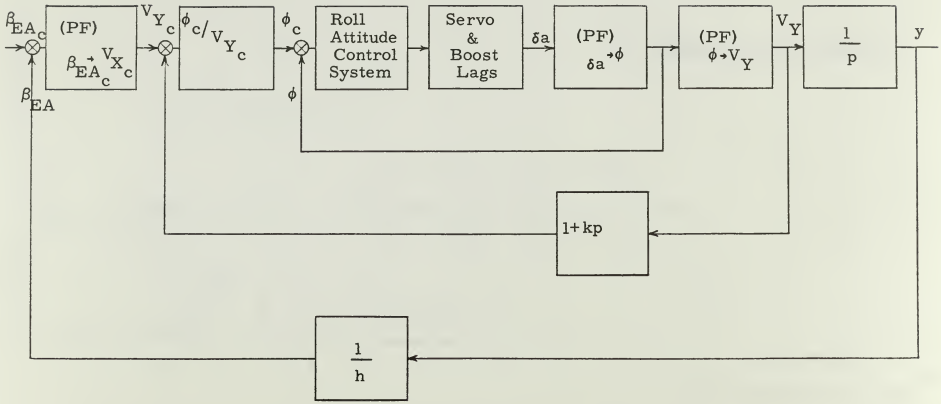

FIG. 25 MATHEMATICAL BLOCK DIAGRAM OF THE LATERAL CONTROL CHANNEL

of the angle, is the command signal since β_{EA}, compared with a_{EA}, is small during the approach. The performance functions for the landing system and for the Velocity Flight Control System, incorporating compensation and servo lags, are shown below.

$$(PF)ol_{\phi_c \rightarrow \delta_a} = \frac{5730\ (p+1.22)}{(p+12.2)\ (p+10.0)\ (p+15.15)} \tag{4-20}$$

(Approach)

$$(PF)ol_{\beta_{EA_c} \rightarrow V_{Y_c}} = \frac{4.64(p+.444)\ (p+.056)}{p\ (p+1.0)} \tag{4-21}$$

(Landing)

$$(PF)ol_{\beta_{EA_c} \rightarrow V_{Y_c}} = \frac{25.52(p+.0455 \pm j.0497)}{p\ (p+1.0)} \tag{4-22}$$

No attempt is made here to establish limits for aircraft and ship roll angles that will permit a safe landing. Such a limit must be established, however, for a particular aircraft. A study has shown that the roll of a destroyer will not exceed 5 degrees[3] two thirds of the time. A ship roll angle of 10 degrees and an aircraft roll angle of 5 degrees are taken here to be maximum values. The center of landing area is on the center line of the ship 30 feet above the center of gravity. Roll of the ship is simulated by sinusoids with frequencies of 1 and 1/2 radians per second. This frequency range includes the natural frequency[3] of a destroyer. The beam of a destroyer is approximately 40 feet and a landing within 10 feet of the center of the landing area is considered acceptable. As shown in Fig. 24, the command signal is limited such that ϕ will not exceed 5 degrees during the final descent. Limiting ϕ also insures stability

in the final phase of the approach. An integrated by-pass signal is used as a vernier to eliminate any steady state error.

Analog simulation showed that the system would track the center of the landing area with a maximum error in y of six feet (Figs. 26 and 27). To reduce this error, it was suggested that a signal be assumed available from an accelerometer mounted on the deck and aligned with the lateral axis of the ship. This signal was used to augment the command in V_{Y_A} and the limit on $V_{Y_{A_C}}$ was removed. Fig. 28 shows that the aircraft could be positioned with a maximum error in y of less than 1 foot, but that aircraft roll angles of 26 degrees were required. With $V_{Y_{A_C}}$ again limited so as to restrict ϕ, Fig. 29 shows that the maximum error in y will exceed 4 feet.

Fig. 30 shows the response of the lateral system with the aircraft initially 500 feet from the ship and 15 feet from the approach radial. Initial $V_{(E-A)_{X_A}}$ is 40 knots. The approach is made with a crosswind of 3.5 knots to show the trim roll angle required.

Hence, the results of analog simulation show that a successful landing can be made by commanding the aircraft velocity with signals proportional to the vector angles in the Earth-Aircraft coordinate frame.

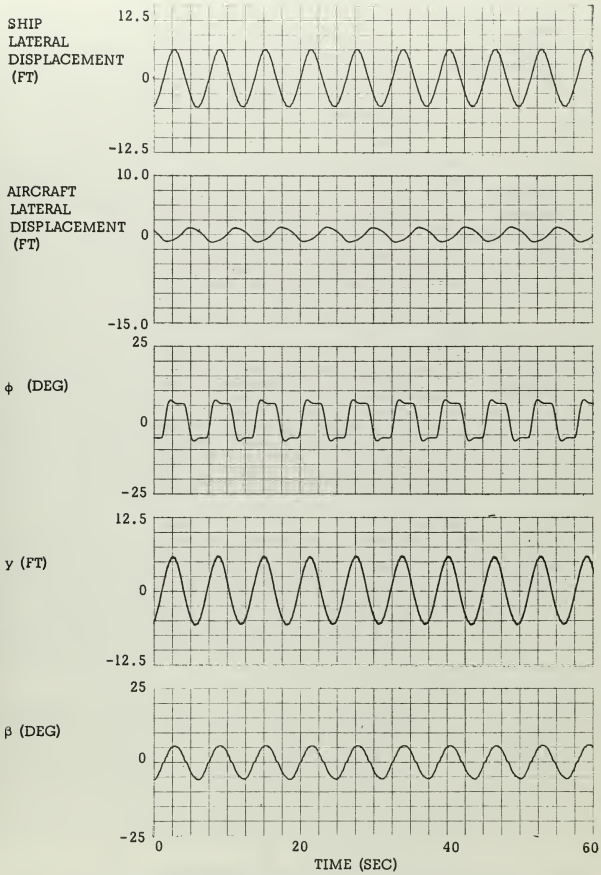

FIG. 26 RESPONSE OF THE LATERAL SYSTEM IN HOVER FLIGHT OVER THE SHIP - h = 50 FEET - SHIP ROLL FREQUENCY OF 1 RADIAN/SEC - V_Y LIMITED AND COMMANDED BY β.

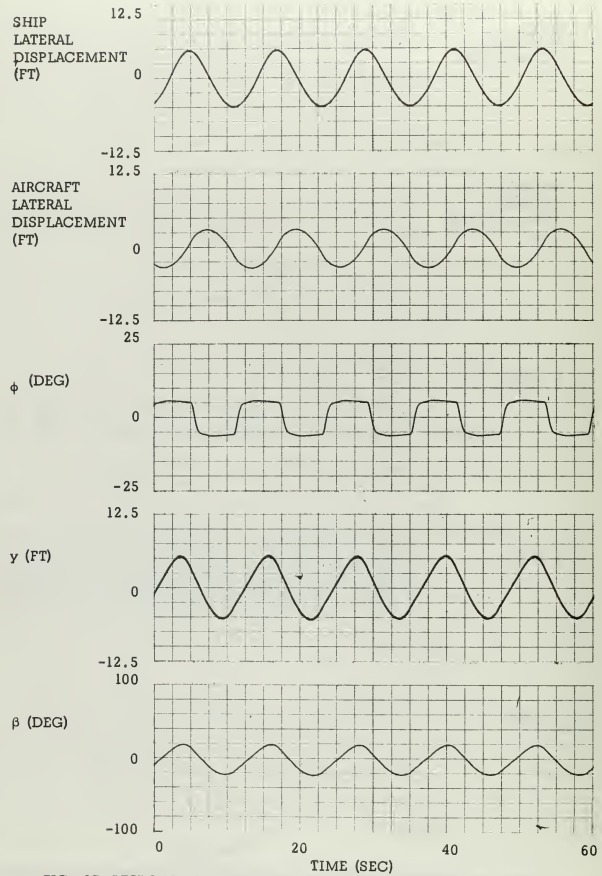

FIG. 27 RESPONSE OF THE LATERAL SYSTEM IN HOVER FLIGHT OVER THE SHIP - h = 12 FEET - SHIP ROLL FREQUENCY OF 1/2 RADIAN/SEC - V_Y LIMITED AND COMMANDED BY β.

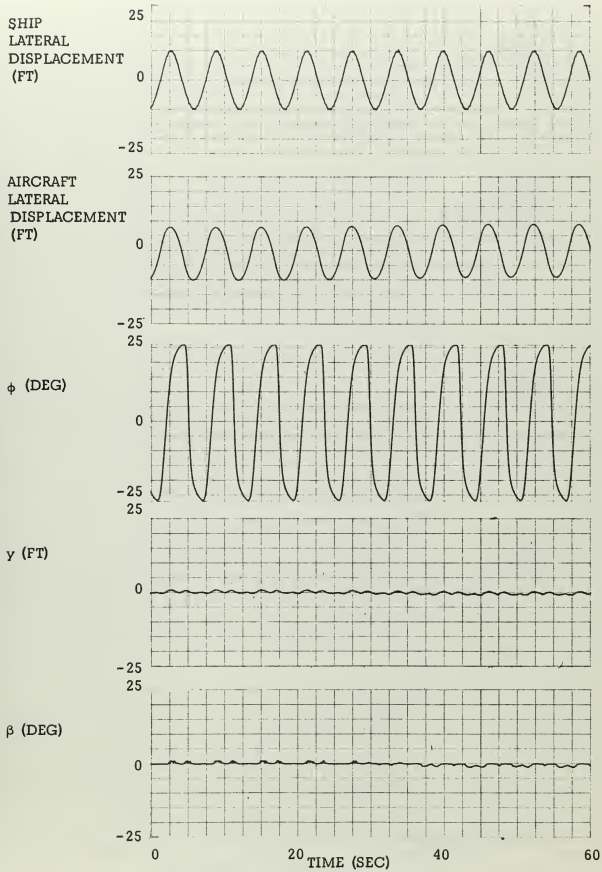

FIG. 28 RESPONSE OF THE LATERAL SYSTEM IN HOVER FLIGHT OVER THE SHIP - h = 50 FEET - SHIP ROLL FREQUENCY OF 1 RADIAN/SEC - V_Y UNLIMITED AND COMMANDED BY LATERAL SHIP ACCELERATION.

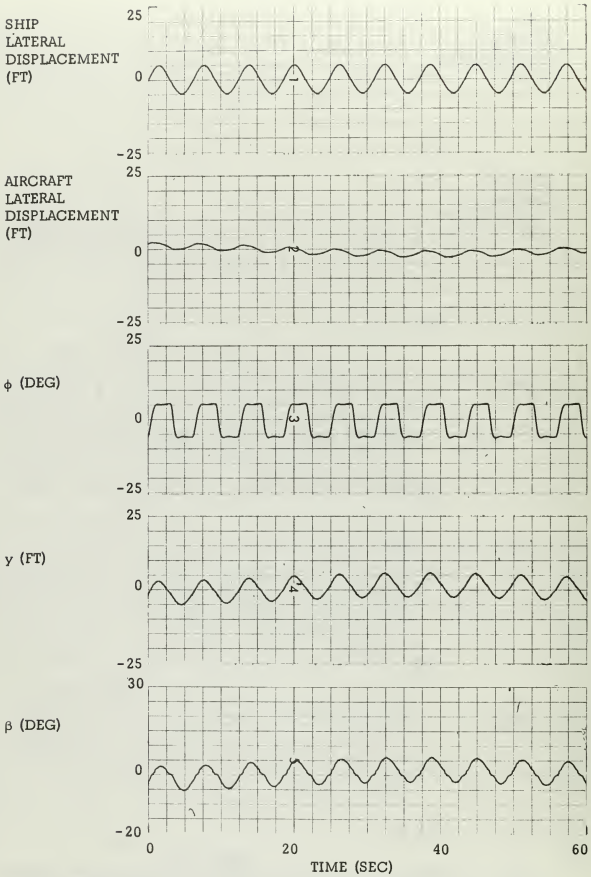

FIG. 29 RESPONSE OF THE LATERAL SYSTEM IN HOVER FLIGHT OVER THE SHIP - h = 50 FEET - SHIP ROLL FREQUENCY OF 1 RADIAN/SEC - V_y LIMITED AND COMMANDED BY LATERAL SHIP ACCELERATION.

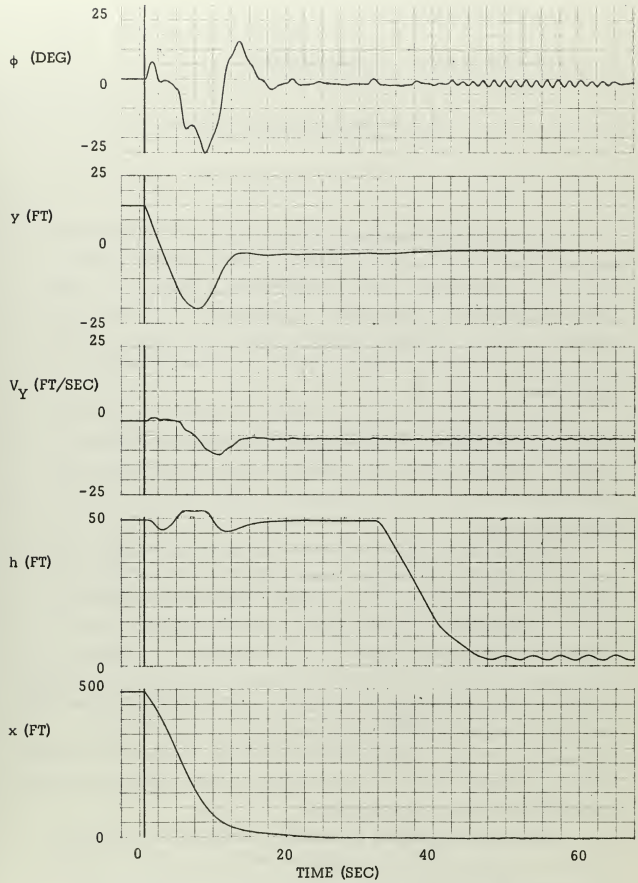

FIG. 30 RESPONSE OF THE LATERAL SYSTEM IN A CROSS-WIND APPROACH
x_0 = 500 FEET - y_0 = 15 FEET

CHAPTER V

THE VECTOR TRACKING SENSOR

It has been presumed that the vector from the aircraft to the intended point of landing can be tracked and that signals, proportional to the angles which define the direction of the vector in the aircraft body frame, are available to command the velocity of the aircraft. It is not the purpose of this study to instrument the sensor. A brief discussion of how the vector might be tracked is appropriate.

A non-directional source of energy emission at the center of the landing platform, with a passive tracking element in the aircraft, appears to be the most direct means of instrumentation. The radiation may be in the infra-red or radar range of the frequency spectrum.

Infra-red sensors and emitters are relatively simple, inexpensive, and light. The emitter must radiate significantly more energy per unit area than other sources of infra-red radiation on the ship. Identification of the source at the landing point can be assured by filtering the frequency and modulating the intensity of radiation. Infra-red radiation, as a means of defining the vector, has several disadvantages. It is subject to atmospheric scattering[9] and also to attenuation[10] by water vapor in the atmosphere. Instrumenting with IR would give the aircraft the capability of making "blind" landings in forward combat areas at night, since the source of radiation is easily transportable.

Radar can provide the all weather capability for the system. Aircraft fire control systems use a combination of radar and infra-red detectors[10] to track a vector. The radar is used for target

acquisition and course tracking. The infra-red sensor provides finer angular coordinate information.

Use of both inf ra-red and radar trackers would provide the landing system with the the means of meeting the requirements defined in Chapter II.

CHAPTER VI

CONCLUSIONS AND RECOMMENDATIONS FOR FURTHER STUDY

CONCLUSIONS

A control system which will land VTOL aircraft on small ships underway is feasable. By tracking the line of sight vector from the aircraft to the ship, signals, proportional to the angles which define the vector in the Earth-Aircraft coordinate frame, can be generated. Using these signals to command a Velocity Flight Control System, the aircraft can be positioned over the deck for landing. Prior knowledge of the height of the landing platform and the direction of the wind over the deck, within the accuracy of the ship's weather vane are required. It is not necessary for the pilot to know the course or speed of the ship.

The dynamics of the ship have a significant effect upon the design of the landing system. The vertical motion of a ship is caused primarily by pitch and heave. By locating the landing area between 1/2 and 2/3 of the length of the ship aft of the bow, the effect of these motions on the landing aircraft can be minimized. The maximum vertical velocity of the landing area can be statistically predicted. The vertical velocity of the aircraft can then be commanded independently of the motions of the ship so as not to exceed the structural limitations of the landing gear when contact with the deck is made.

The design of the landing gear also requires that the attitude of the aircraft, with respect to the deck, at the time of landing be limited. Roll of the deck is more critical than pitch. Roll can be minimized by heading the ship into the waves or significantly reduced by mechanically roll stabilizing the ship. The aircraft attitude must be restricted to small angles at the time of landing. This is accomplished by limiting the pitch and roll command signals. These limited signals

are sufficient for the aircraft to follow the translation of the ship.

With the necessary limits on the aircraft attitude, it is not possible to hold the aircraft over the instantaneous position of the center of a rolling deck. By commanding the aircraft velocity with the vector angles, a landing can be made within 6 feet of the desired touchdown point on a ship rolling 10 degrees. The landing error can be reduced to less than 1 foot by commanding the aircraft velocity with signals from an accelerometer mounted on the deck of the ship, but aircraft roll angles of 26 degrees are required. With the aircraft attitude limited, the maximum landing error is 4 feet using the acceleration commands. With the attitude limits imposed, the aircraft will tend to remain over the mean, rather than the instantaneous, position of the desired landing point whether the aircraft velocity is commanded by ship acceleration or by vector angles.

By commanding velocity with the vector angles, position feedback is provided for the Velocity Flight Control System but the entire system is unstable in the final approach. Limiting the aircraft attitude commands provides the necessary stability.

The landing system requires a non-directional emitter of radiant energy on the landing deck. A sensor, mounted in the aircraft, tracks the line of sight vector to the energy source and provides the vector angles necessary to command the aircraft velocity.

The Velocity Flight Control System is an integral and necessary part of the landing system. It provides the Euler Angles for the coordinate transformation of the line of sight vector to the Earth-Aircraft frame. By commanding the aircraft velocity in an earth fixed rather than an air mass coordinate frame, the time required to make the landing approach is not a function of the air mass velocity. Finally, since the Velocity Flight Control System is relatively insensitive to wind gust, the effect of turbulence in the landing approach is minimized.

RECOMMENDATIONS FOR FURTHER STUDY

Since the aircraft cannot be held directly over the desired point of landing at all times during the descent, a lateral velocity of the aircraft with respect to the deck will exist at the time of landing. An acceptable tolerance on this velocity is an area for further study.

An investigation of how to best instrument the tracking sensor is also a subject for additional study.

APPENDIX A

SUMMARY OF THE METHOD USED FOR DETERMINING THE PROBABILITY OF VERTICAL SHIP MOTION

This is a summary of the method contained in Ref. 6 for determining the probability of vertical ship motion. The method is used in Chapter III to determine the probability of occurrence of vertical velocity at a particular deck station.

The ship motions are described in two uncoupled, second order equations. Coefficients defining mass, damping, forcing and restoring forces and moments are developed. These are either derived analytically or are obtained emperically. The surface of the ocean can be described in terms of a spectrum of wave frequencies and the wave heights have a normal or Gauss-LaPlace distribution in a given sea state. The waves in a given sea state have a dominant frequency or period which is a function of prior wind conditions. Therefore, the wave forcing function is assumed to be characterized by a sinusoid of the predominant frequency, and the ship response function is computed. The ship model used approximated the hull shape of a destroyer and the analysis was conducted with the ship at the verge of slamming. The result is a transfer function for the ship that gives the maximum vertical motion per foot of wave height along the slamming boundary.

Waves are generated by wind and a given wind is capable of producing wave lengths up to a certain maximum. This wind must exist for a relatively long period of time to fully develop the wave lengths. Analytical methods have been developed for describing the surface of the ocean which correlate well with the fully developed sea. The fully developed sea associated with one wind velocity

seldom exist. Therefore, the probability of occurrence of waves of a particular frequency and amplitude was determined from emperical data taken in the North Atlantic. With the statistical probability of wave occurrence and the specific transfer function already developed, the probability of ship response was determined.

Figs. A-1, A-2, A-3, A-4, and A-5 are reproduced from Ref. 3. The data presented is for ships 400 and 600 feet long steaming into the waves at 10 and 20 knots. Fig. A-1 shows the percent of all time that the ship can be brought to the slamming boundary. Figs. A-2 and A-3 show the probability of pitch angle. Figs. A-4 and A-5 show the probability of heave rate or vertical velocity of the ship center of gravity. Figs. A-6 and A-7, showing pitch rate, were obtained by identical methods. Data contained in these curves is used in the calculations of Chapter III.

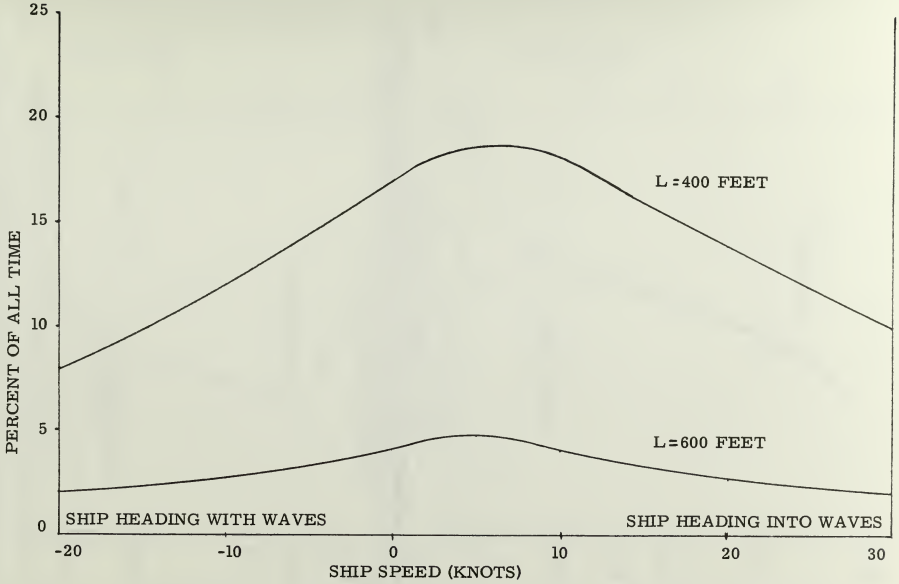

FIG. A-1 PERCENTAGE OF TIME THAT A SHIP OF LENGTH "L" CAN BE BROUGHT TO A SLAMMING CONDITION (ADAPTED FROM REF. 6)

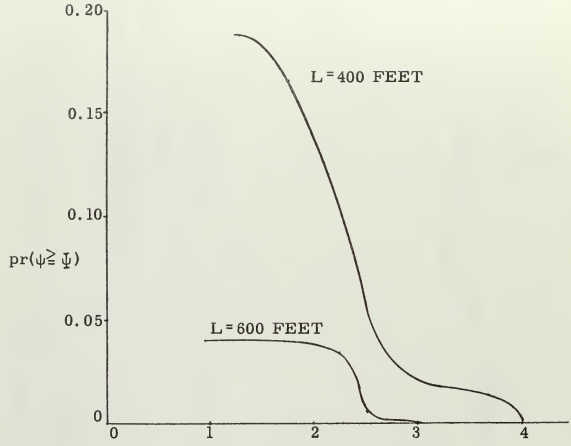

FIG. A-2 PROBABILITY pr ($\psi \geqq \Psi$) THAT PITCH ANGLE IS EQUAL EQUAL TO OR GREATER THAN Ψ SHIP INTO WAVES AT 10 KNOTS (ADAPTED FROM REF. 6)

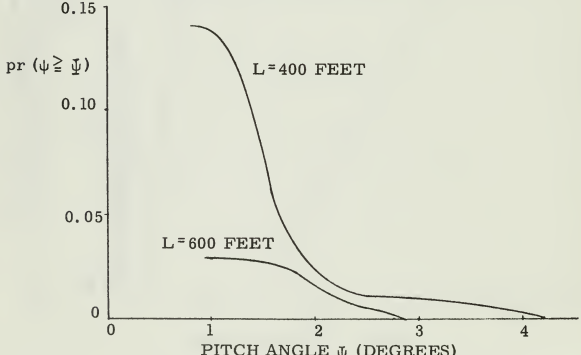

FIG. A-3 PROBABILITY pr($\psi \geqq \Psi$) THAT PITCH ANGLE IS EQUAL TO OR GREATER THAN Ψ SHIP INTO WAVES AT 20 KNOTS (ADAPTED FROM REF 6.)

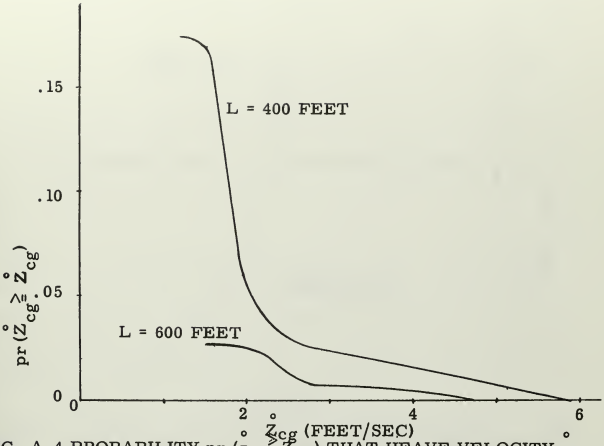

FIG. A-4 PROBABILITY pr ($z_{cg} \geq Z_{cg}$) THAT HEAVE VELOCITY z_{cg} IS EQUAL TO OR GREATER THAN Z_{cg} - SHIP HEADING INTO WAVES AT 10 KNOTS (ADAPTED FROM REF. 6)

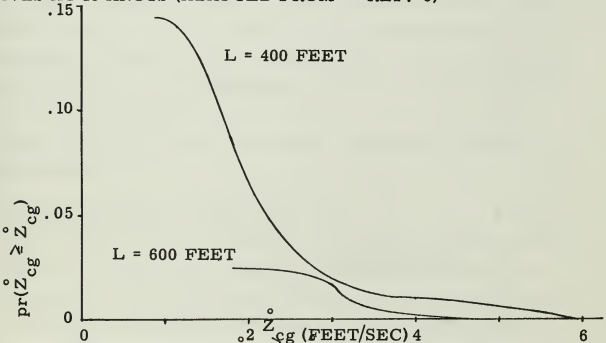

FIG. A-5 PROBABILITY pr ($z_{cg} \geq Z_{cg}$) THAT HEAVE VELOCITY z_{cg} IS EQUAL TO OR GREATER THAN Z_{cg} - SHIP HEADING INTO WAVES AT 20 KNOTS (ADAPTEF FROM REF. 6)

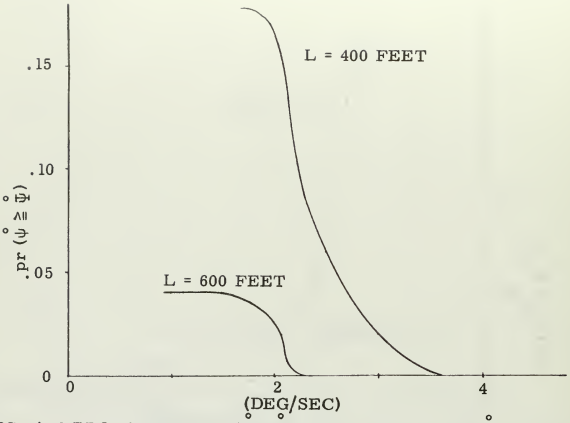

FIG. A-6 PROBABILITY pr ($\dot{\psi} \geq \dot{\Psi}$) THAT PITCH RATE $\dot{\psi}$ IS EQUAL TO OR GREATER THAN $\dot{\Psi}$ - SHIP HEADING INTO WAVES AT 10 KNOTS

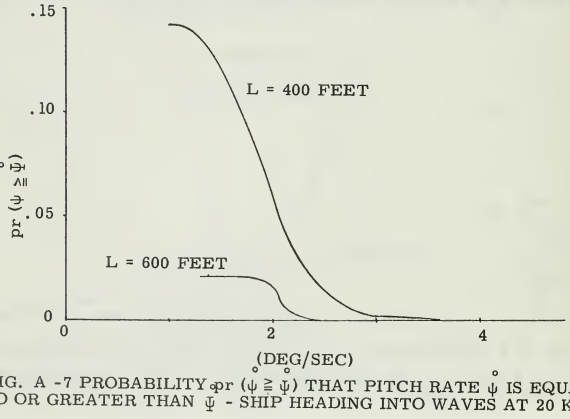

FIG. A -7 PROBABILITY pr ($\dot{\psi} \geq \dot{\Psi}$) THAT PITCH RATE $\dot{\psi}$ IS EQUAL TO OR GREATER THAN $\dot{\Psi}$ - SHIP HEADING INTO WAVES AT 20 KNOTS

APPENDIX B

COORDINATE FRAMES AND EQUATIONS OF MOTION

The basis for the equations describing the motion of an aircraft is Newton's second law which states that the net force equals the mass times the acceleration. This is experimentally true only in an inertial frame. An inertial frame is a frame in which Newton's first law holds that a particle, free from forces, is unaccelerated. Forces acting on an aircraft are normally described in a frame fixed to the aircraft and therefore rotating with respect to an inertial frame. Further, many of these forces are developed from motion of the aircraft with respect to the air mass, and generally motions of the aircraft with respect to the earth are desired. The requirements for several coordinate frames is clear if equations are to completely and accurately describe the motion of the aircraft.

There are six coordinate frames used in this study. These are described below.

a. Inertial Coordinate Frame (I) X_I, Y_I, Z_I

An inertial frame is one which is not rotating or accelerating with respect to inertial space. In general the solar system may be considered to form such a frame. However, since the acceleration of the center of the earth with respect to inertial space is small compared to other accelerations involved, the location of the origin of the Inertial Coordinate Frame is placed at the center of the earth. This frame is nonrotating, with the Z_I axis coincident

with the rotational axis of the Earth. The X_I and Y_I axes then lie in the equatorial plane.

b. Earth Centered Coordinate Frame (E) X_E, Y_E, Z_E

This frame is fixed with respect to the Earth with its origin at the center of the Earth. The Z_E axis is coincident with the Z_I axis and the Earth's rotational axis. The X_E and Y_E axes lie in the equatorial plane intersecting the surface of the Earth at convenient points. The E frame may be chosen to coincide with the I frame at a particular instant of time.

c. Earth Local Vertical Frame (L) X_L, Y_L, Z_L

The Earth Local Vertical Frame is a geographic frame. The origin of this frame is at the center of mass of the aircraft with Z_L along the vertical defined by the local gravity vector (positive downward), X_L parallel to geographic North (positive to the North), and Y_L parallel to geographic East (positive to East).

d. Aircraft Body Coordinate Frame (A) X_A, Y_A, Z_A

The Aircraft Body Coordinate Frame is centered at the center of the mass of the aircraft. The A frame is fixed to the aircraft and rotates and translates with the aircraft. The X_A axis is chosen in a convenient forward direction in the plane of symmetry, the Y_A axis normal to the plane of symmetry (positive to the right), and the Z_A axis in the plane of symmetry (positive downward) forming an orthogonal right-hand system. The alignment used for the X_A axis of the Tandem Rotor Helicopter is a "waterline" axis approximately parallel to the floor.

e. Earth Aircraft Coordinate Frame (EA), X_{EA}, Y_{EA}, Z_{EA}

The Earth-Aircraft Coordinate Frame is centered at the center of mass of the aircraft. The Z_{EA} axis is along the local gravity vector (positive downward) and is coincident with the Z_L axis. The X_{EA} axis is the intersection of the horizontal plane with the vertical plane containing the X_A axis. The Y_{EA} axis forms a right-hand system.

f. Air Mass Coordinate Frame (AM) X_{AM}, Y_{AM}, Z_{AM}

The Air Mass Coordinate Frame is oriented parallel to the Earth Local Vertical Frame. The origin of this frame is fixed in the airmass.

Because of the short time periods and relatively small velocities involved in this investigation, the Coriolis and centripetal accelerations due to the earth's rotation are neglected. With this assumption, the E frame becomes the inertial reference frame for Newton's law. Further, if it is assumed that the air mass translates with constant speed with respect to the Earth the following is then true:

$$\bar{a}_{(I-A)} = \bar{a}_{(E-A)} = \bar{a}_{(AM-A)} \tag{B-1}$$

Since it is desired to have the components of acceleration along the axes of the rotating A frame, this becomes:

$$\bar{a}_{(I-A)} = \left[\frac{d\bar{V}_{(I-A)}}{dt} \right]_I = \left[\frac{d\bar{V}_{(I-A)}}{dt} \right]_A + \bar{W}_{(I-A)} \times \bar{V}_{(I-A)} \tag{B-2}$$

The subscript on the derivative indicates the vector components are in the A or I Frame.

Now applying Newton's law to the vehicle, which has numerous forces applied, the following equation applies.

$$\sum \bar{F} = m\,\bar{a}_{(I-A)} = m \left[\frac{d\bar{V}_{(I-A)}}{dt} \right]_A + m\,\bar{W}_{(I-A)} \times \bar{V}_{(I-A)} \tag{B-3}$$

In expanding equation (B-3) along the A frame axes

$$\sum F_X = m\, a_{(I-A)_{X_A}} = m\,(\dot{V}_{(I-A)_{X_A}} + W_{(I-A)_{Y_A}} V_{(I-A)_{Z_A}} - W_{(I-A)_{Z_A}} V_{(I-A)_{Y_A}}) \tag{B-4}$$

$$\sum F_Y = m\, a_{(I-A)_{Y_A}} = m\,(\dot{V}_{(I-A)_{Y_A}} + W_{(I-A)_{Z_A}} V_{(I-A)_{X_A}} - W_{(I-A)_{X_A}} V_{(I-A)_{Z_A}}) \tag{B-5}$$

$$\sum F_Z = m\, a_{(I-A)_{Z_A}} = m\,(\dot{V}_{(I-A)_{Z_A}} + W_{(I-A)_{X_A}} V_{(I-A)_{Y_A}} - W_{(I-A)_{Y_A}} V_{(I-A)_{X_A}}) \tag{B-6}$$

Correspondingly, there is a relationship which states that the applied moment equals the vector differentiation of the angular momentum, or sometimes called moment of momentum, of the vehicle with respect to inertial space. This can also be stated as a vector in the A frame by the following

$$\sum \bar{M} = \left[\frac{d\,\bar{I}\bar{W}}{dt}\right]_I = \left[\frac{d\,\bar{I}\bar{W}}{dt}\right]_A + \bar{W}_{(I-A)} \times \bar{I}\bar{W} \tag{B-7}$$

Expanding this to components in the A frame and making the assumption that Y_A is a principle axis, yields

$$\sum L = I_x \dot{W}_{(I-A)_{X_A}} - I_{xz} \dot{W}_{(I-A)_{Z_A}} - I_{xz} W_{(I-A)_{X_A}} W_{(I-A)_{Y_A}} \quad \text{(B-8)}$$

$$+ (I_z - I_y) W_{(I-A)_{Y_A}} W_{(I-A)_{Z_A}}$$

$$\sum M = I_y \dot{W}_{(I-A)_{Y_A}} - I_{xz} (W^2_{(I-A)_{Z_A}} - W^2_{(I-A)_{X_A}}) \quad \text{(B-9)}$$

$$+(I_x - I_z) W_{(I-A)_{X_A}} W_{(I-A)_{Z_A}}$$

$$\sum N = I_z \dot{W}_{(I-A)_{Z_A}} - I_{xz} \dot{W}_{(I-A)_{X_A}} + I_{xz} W_{(I-A)_{Y_A}} W_{(I-A)_{Z_A}} \quad \text{(B-10)}$$

$$+(I_y - I_x) W_{(I-A)_{X_A}} W_{(I-A)_{Y_A}}$$

To facilitate analysis, the above equations of motion are linearized. Linearization of these equations is accomplished by setting each independent variable equal to an initial steady-state value plus a small perturbation term. Steady-state implies that all forces and moments are balanced when all perturbation quantities go to zero. By setting

$$V_{(I-A)_{X_A}} = V_{(I-A)_{X_{Ao}}} + V_{X_A} \quad \text{(B-11)}$$

$$W_{(I-A)_{X_A}} = W_{(I-A)_{X_{Ao}}} + W_{X_A}$$

etc.

and substituting these into equation (B-4) we have

$$F_X = m \left[\dot{V}_{(I-A)_{X_{Ao}}} + \dot{V}_{X_A} + (W_{(I-A)_{Y_{Ao}}} + W_{Y_A})(V_{(I-A)_{Z_{Ao}}} + V_{Z_A}) \right.$$

$$\left. -(W_{(I-A)_{Z_{Ao}}} + W_{Z_A})(V_{(I-A)_{Y_{Ao}}} + V_{(I-A)_{Y_A}}) \right] \tag{B-12}$$

and also

$$F_X = o = m \left[\dot{V}_{(I-A)_{X_{Ao}}} + W_{(I-A)_{Y_{Ao}}} V_{(I-A)_{Z_{Ao}}} - W_{(I-A)_{Z_{Ao}}} V_{(I-A)_{Y_{Ao}}} \right] \tag{B-13}$$

Subtracting equation (B-13) from (B-12) and neglecting higher order terms, the result is

$$F_X = m \left[\dot{V}_{X_A} + W_{(I-A)_{Y_{Ao}}} V_{Z_A} + W_{Y_A} V_{(I-A)_{Z_{Ao}}} \right. \tag{B-14}$$

$$\left. -W_{(I-A)_{Z_{Ao}}} V_{Y_A} - W_{Z_A} V_{(I-A)_{Y_{Ao}}} \right]$$

Further, if the stipulation is made that in this steady state condition the aircraft is not changing attitude, all of the initial W's will be zero, thereby reducing equation (B-14) to

$$F_X = m \left[\dot{V}_{X_A} + W_{Y_A} V_{(I-A)_{Z_{Ao}}} - W_{Z_A} V_{(I-A)_{Y_{Ao}}} \right] \tag{B-15}$$

Similarly we can make this same substitution in equations (-5, 6, 8, 9 and 10) resulting in

$$F_Y = m \left[\dot{V}_{Y_A} + W_{Z_A} V_{(I-A)_{X_{Ao}}} - W_{X_A} V_{(I-A)_{Z_{Ao}}} \right] \tag{B-16}$$

$$F_Z = m\left[\dot{V}_{Z_A} + W_{X_A} V_{(I-A)_{Y_{Ao}}} - W_{Y_A} V_{(I-A)_{X_{Ao}}}\right] \quad \text{(B-17)}$$

$$L = I_x \dot{W}_{X_A} - I_{xz} \dot{W}_{Z_A} \quad \text{(B-18)}$$

$$M = I_y \dot{W}_{Y_A} \quad \text{(B-19)}$$

$$N = I_z \dot{W}_{Z_A} - I_{xz} \dot{W}_{X_A} \quad \text{(B-20)}$$

The quantities making up the force and moment terms consist of aerodynamic forces and moments plus those generated by control inputs. In actuality, many of these terms are quite complicated, but for most types of studies they can be expanded in a series about the initial steady state velocity, keeping only the first order term. The results of this operation are the equations of motion shown below (note that these equations are still in dimensional form and are used in this form).

$$F_x = m\left[\dot{V}_{X_A} + W_{Y_A} V_{(I-A)_{Z_{Ao}}} - W_{Z_A} V_{(I-A)_{Y_{Ao}}}\right] = X_{V_X} V_{X_A}$$

$$+ X_q W_{Y_A} + X_{V_Z} V_{Z_A} + X_{\delta e}\delta e + X_{\delta z}\delta z - (mg \cos E_o)\Delta E \quad \text{(B-21)}$$

$$F_y = m\left[\dot{V}_{Y_A} + W_{Z_A} V_{(I-A)_{X_{Ao}}} - W_{X_A} V_{(I-A)_{Z_{Ao}}}\right] = Y_p W_{X_A}$$

$$+ Y_r W_{Z_A} + Y_{V_Y} V_{Y_A} + Y_{\delta r}\delta r + Y_{\delta a}\delta a + (mg \cos E_o)\phi \quad \text{(B-22)}$$

$$F_z = m\dot{V}_{Z_A} + W_{X_A} V_{(I-A)_{Y_{Ao}}} - W_{Y_A} V_{(I-A)_{X_{Ao}}} = Z_{V_X} V_{X_A}$$

$$+ Z_q W_{Y_A} + Z_{V_Z} V_{Z_A} + Z_{\delta e}\delta e + Z_{\delta z}\delta z - (mg \sin E_o)\,\Delta E \qquad \text{(B-23)}$$

$$L = I_x \dot{W}_{X_A} - I_{xz} \dot{W}_{Z_A} = L_p W_{X_A} + L_r W_{Z_A}$$

$$+ L_{V_Y} V_{Y_A} + L_{\delta r}\delta r + L_{\delta a}\delta a \qquad \text{(B-24)}$$

$$M = I_y \dot{W}_{Y_A} = M_{V_X} V_{X_A} + M_q W_{Y_A} + M_{V_Z} V_{Z_A}$$

$$+ M_{\delta e}\delta e + M_{\delta z}\delta z \qquad \text{(B-25)}$$

$$N = I_z \dot{W}_{Z_A} - I_{xz} \dot{W}_{X_A} = N_p W_{X_A} + N_r W_{Z_A}$$

$$+ N_{V_Y} V_{Y_A} + N_{\delta r}\delta r + N_{\delta a}\delta a \qquad \text{(B-26)}$$

The force amd moment coefficients for the Vertol 107 at an air mass velocity of 40 knots are shown in Tables B-I and B-II. Gross weight and moments of inertia are given below.

$mg = 13{,}600$ lbs

$I_x = 7{,}460$ slug ft^2

$I_y = 57{,}800$ slug ft^2

$I_z = 54{,}200$ slug ft^2

$I_{xz} = 5{,}420$ slug ft^2

The linearized equations of motion are programmed in their entirety for analog simulation with these parameters. The equations are also used to derive the aircraft performance functions in Chapter IV.

TABLE B-I

FORCE COEFFICIENTS LINEARIZED AT 40 KNOTS

PARAMETER	VALUE	UNITS
X_{V_X}	-19.2	lbs/fps
X_q	-407	lbs/rad per sec
X_{V_Z}	-4.43	lbs/fps
$X_{\delta e}$	+175	lbs/in
$X_{\delta z}$	-4000	lbs/rad
Y_P	-1180	lbs/rad per sec
Y_r	-9.2	lbs/rad per sec
Y_{V_Y}	-31.9	lbs/fps
$Y_{\delta r}$	+133	lbs/in
$Y_{\delta a}$	+740	lbs/in
Z_{V_X}	-117	lbs/fps
Z_q	-1650	lbs/rad per sec
Z_{V_Z}	-266	lbs/fps
$Z_{\delta e}$	+283	lbs/in
$Z_{\delta z}$	-116,000	lbs/rad

Table B-II

FORCE COEFFICIENTS LINEARIZED AT 40 KNOTS

PARAMETER	VALUE	UNITS
L_p	-8500	ft-lbs/rad per sec
L_r	+280	ft-lbs/rad per sec
L_{V_Y}	-133.6	ft-lbs/fps
$L_{\delta r}$	- 1930	ft-lbs/in
$L_{\delta a}$	+5500	ft-lbs/in
M_{V_X}	-895	ft-lbs/rad per sec
M_q	-112,000	ft-lbs/rad per sec
M_{V_Z}	+1390	ft-lbs/fps
$M_{\delta e}$	+25,000	ft-lbs/in
$M_{\delta z}$	+218,000	ft-lbs/rad
N_p	-880	ft-lbs/rad per sec
N_r	-2480	ft-lbs/rad per sec
N_{V_Y}	-152	ft-lbs/fps
$N_{\delta r}$	16,000	ft-lbs/in
$N_{\delta a}$	+1800	ft-lbs/in

APPENDIX C

The Velocity Flight Control System

The information presented in this appendix is from Reference 1. It is presented here since it describes the control system which is commanded by the Vector Angle Command System.

The Velocity Flight Control System is currently being developed by the MIT Instrumentation Laboratory under U. S. Army contract which includes flight testing in a Vertol 107(CH-46) helicopter. The first effort of the Instrumentation Laboratory was to determine the general characteristics of an optimum control system. They examined several types of control responses for several flight conditions. Based on studies using a fixed based flight simulator, it was found that during hovering and low-speed flight a system which would give a linear velocity response to a control displacement increased the precision of control and at the same time greatly reduced the pilot's manipulative and interpretive tasks. It was further found that the velocity response should be the velocity with respect to the Earth rather than with respect to the air mass. Use of this type of velocity feedback substantially eliminates the effects of gusts with the result that the same ease of control is obtained under all atmospheric conditions. The study also showed that in the cruise regime, angular displacement response was superior, and a transition phase would have to be included. Since the flight regime for this study would be slow speed to hover, only the velocity response system is described.

Although the Instrumentation Laboratory is still conducting their study to obtain the optimum control system, the most current system information available is used and is described below.

A block diagram of the longitudinal flight control system is shown in Fig. C - 1. The ratios of the command to the feedback signals are as follows:

$$\frac{E_c}{V_{x_c}} = -1.44 \text{ deg/ft per sec}$$

$$\frac{E_c}{\dot{V}_{x_c}} = .876 \text{ deg/ft per sec}^2$$

$$\frac{\delta e}{E_c} = .05 \text{ in/deg}$$

$$\frac{\delta z}{h} = .390 \text{ in/ft}$$

$$\frac{\delta z}{\dot{h}} = .323 \text{ in/ft per sec}$$

The signal modifier in the longitudinal velocity control system consists of an integral bypass with lead-lag network giving a transfer function as:

$$\frac{\delta e}{E_c}\left[\frac{K(1+a\tau p)}{1+\tau p} + \frac{1}{p}\right]$$

where $\tau = .06$ sec

$a = 10$

$K = 4.2$

The limiter used in the longitudinal velocity channel limited the attitude command to 20 degrees nose up and 5 degrees nose down. Also incorporated in the pitch moment control servo was a rate of control movement

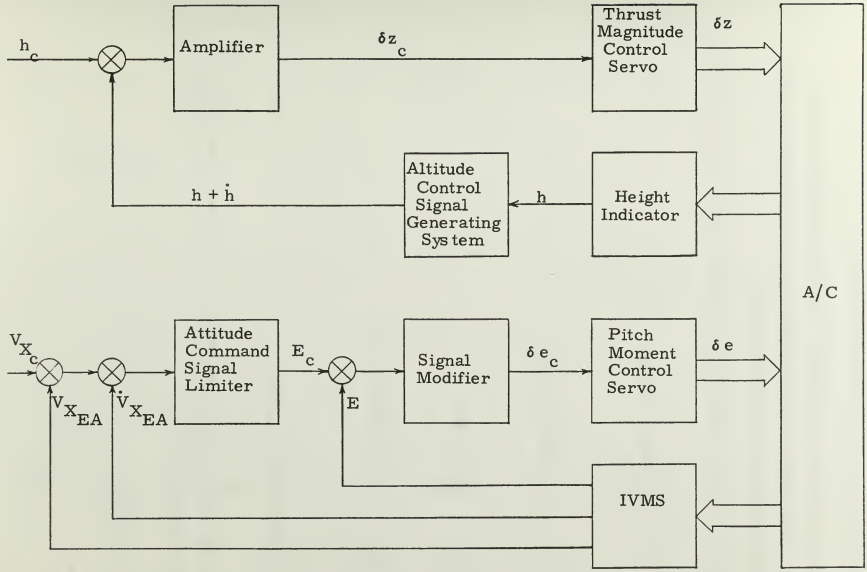

FIG. C-1 FUNCTIONAL BLOCK DIAGRAM OF THE LONGITUDINAL VELOCITY FLIGHT CONTROL SYSTEM

limiter which limited to 7.2 inches per second. The transfer functions of the servos are covered in another paragraph.

The block diagram of the lateral flight control system is shown in Fig. C-2. The lateral velocity control system is very similar to that of the longitudinal velocity control system.

The ratios of the command to the feedback signals are as follows:

$$\frac{\phi_c}{V_{y_c}} = 2.0 \text{ deg/ft per sec}$$

$$\frac{\phi_c}{\dot{V}_{y_c}} = .30 \text{ deg/ft per sec}^2$$

$$\frac{\delta a}{\phi_c} = .066 \text{ in/deg}$$

$$\frac{\delta r}{W_{Z_c}} = .197 \text{ in/deg per sec}$$

$$\frac{W_{Z_c}}{H_c} = .54 \text{ deg per sec/deg}$$

The signal modifier in the roll attitude control system consist of a lead-lag network of the form

$$\frac{1 + a\tau p}{1 + \tau p}$$

where $\tau = .082$ sec

$a = 10$

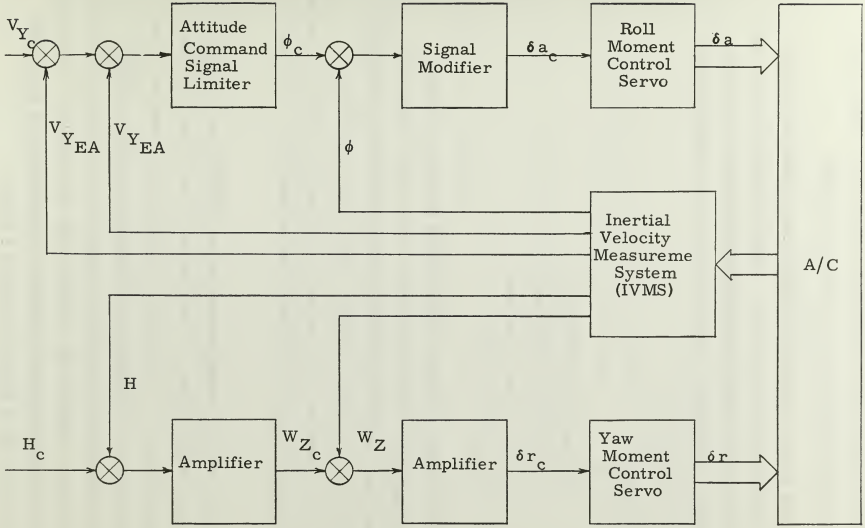

FIG. C-2 FUNCTIONAL BLOCK DIAGRAM OF THELATERAL VELOCITY FLIGHT CONTROL SYSTEM

The roll attitude command signal was limited to $\pm$30 degrees. Again the roll moment control servo incorporated a control rate limiter which limited the control movement to 7.2 inches per second.

The control system and helicopter have four dynamic lags which must be incorporated in the simulation. These are the MIT servo, the lower boost servo, the upper boost servo and the rotor system itself. It was confirmed by tests that each of these could be represented by a first order lag of the form

$$\frac{1}{1 + \tau p}$$

where τ = .066 sec for the MIT servo
τ = .01 sec for the lower servo
τ = .01 sec for the upper servo
τ = .06 sec for the rotor

Each of the four control channels contain these four lags. A short root locus investigation shows that if the τ's are small, that two or more of these lags could be combined into one lag with the same effect on the system by setting the combined τ equal to the sum of the individual τ's. Therefore, for simulation purposes the upper and lower boost servo and the rotor were combined and a conservative τ of .1 sec was used.

The Inertial Velocity Measurement System (IVMS) is an inertial package whose stable element is instrumented to be aligned with the Local Vertical Frame (L). It is capable of providing the velocity of the aircraft with respect to the earth and providng the orientation of the Aircraft Body Coordinate Frame (A) with respect to the L frame in the form of the Euler angles; Heading (H), Elevation (E), and Roll (ϕ). With these Euler angles the system has the capability of performing the coordinate transformation from the A frame to the EA or L frames.

APPENDIX D

ANALOG COMPUTER SIMULATION

The details of analog computer simulations are shown in this appendix. The following symbols are used:

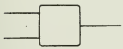
Amplifier used as summer or inverter

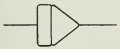
Integrator

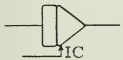

Integrator with an initial condition


Coefficient potentiometer

Amplifier with limited output

Signal limiter (no sign change)

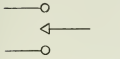
Switch (These are switched on final descent)

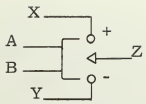

Comparator: If A + B > o then X → Z
If A + B < o then Y → Z

PACE and REAC analog computers were used for the simulation. The subscript A, indicating components in the aircraft body frame, is deleted from these diagrams.

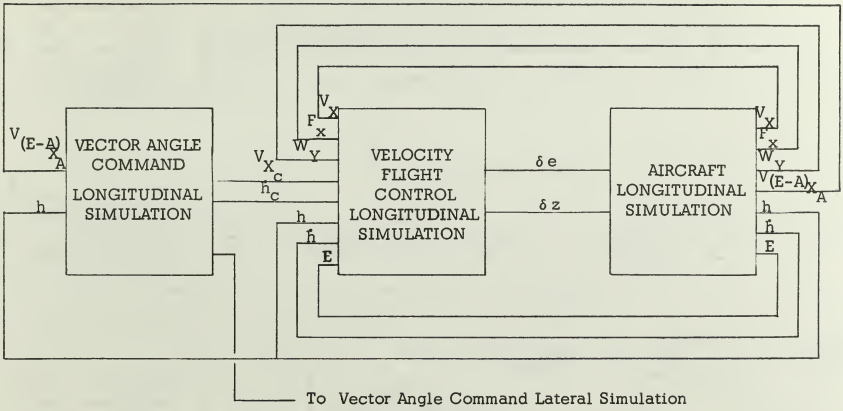

FIG. D-1 BLOCK DIAGRAM OF LONGITUDINAL SIMULATION

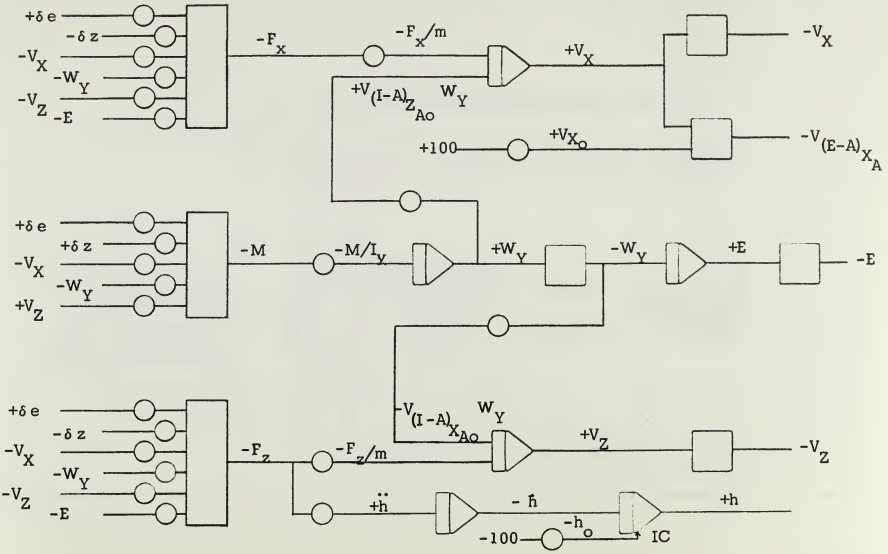

FIG. D-2 AIRCRAFT LONGITUDINAL SIMULATION

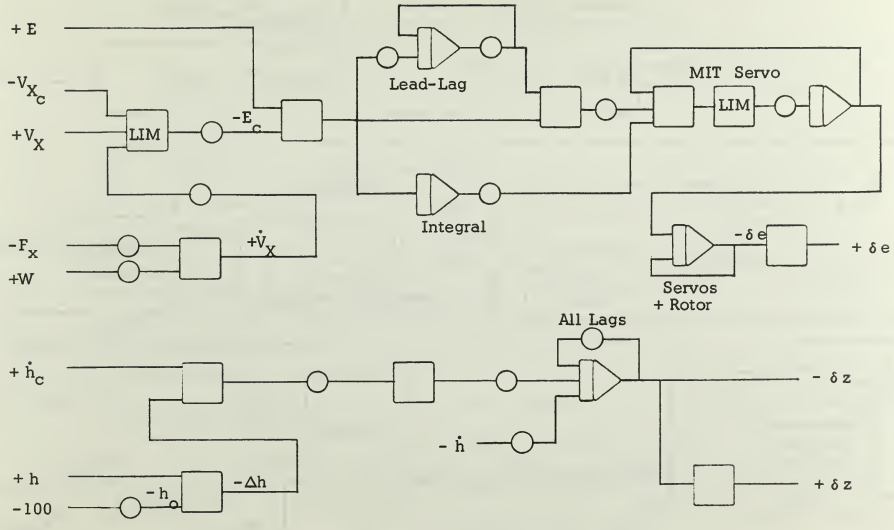

FIG. D-3 VELOCITY FLIGHT CONTROL LONGITUDINAL SIMULATION

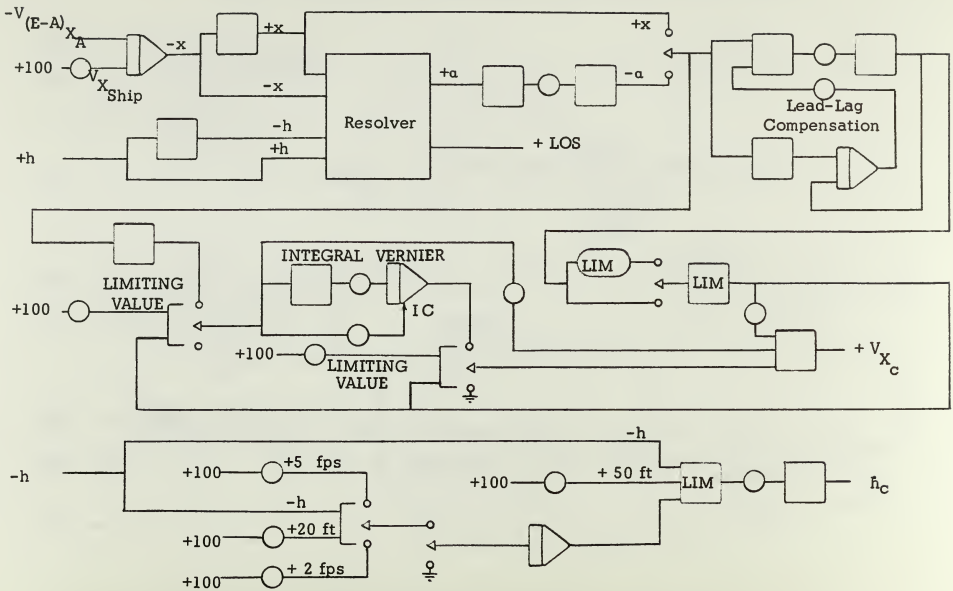

FIG. D-4 VECTOR ANGLE COMMAND LONGITUDINAL SIMULATION

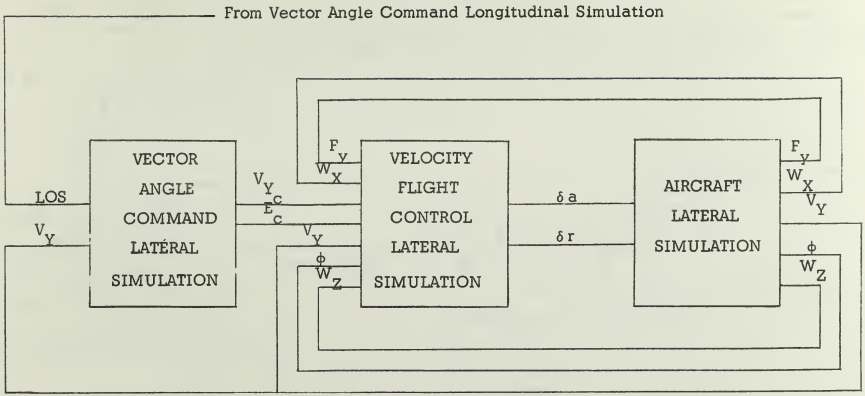

FIG. D-5 BLOCK DIAGRAM OF LATERAL SIMULATION

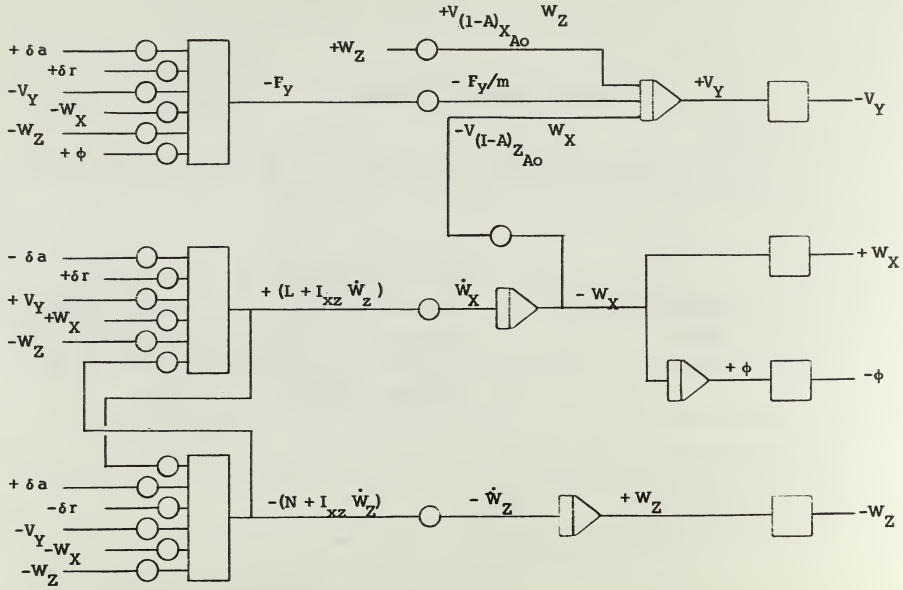

FIG. D-6 AIRCRAFT LATERAL SIMULATION

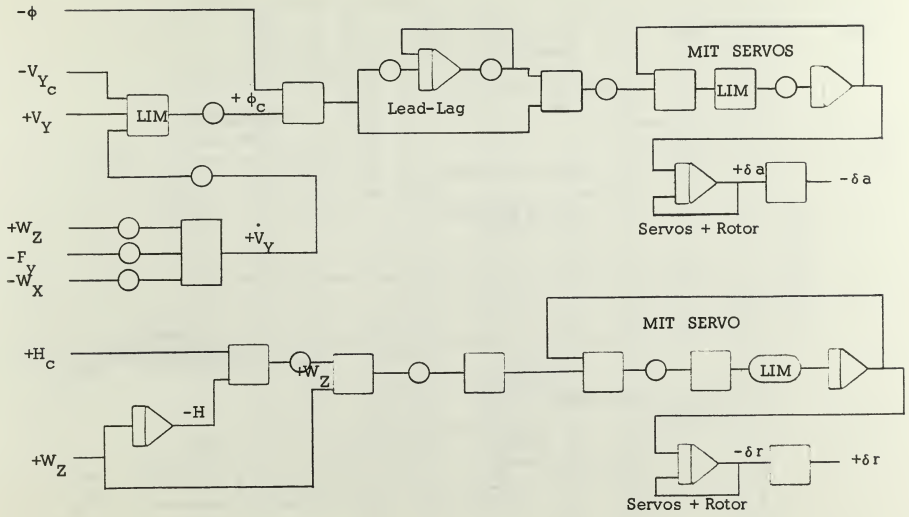

FIG. D-7 VELOCITY FLIGHT CONTROL LATERAL SIMULATION

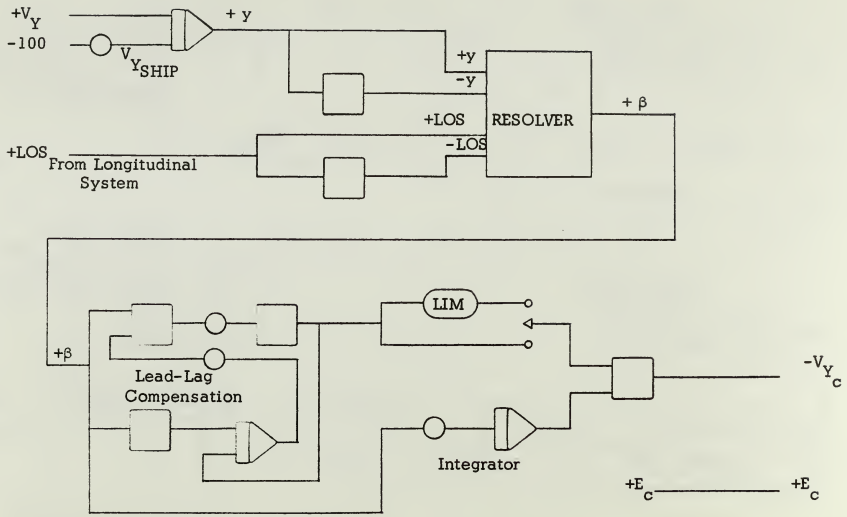

FIG. D-8 VECTOR ANGLE COMMAND LATERAL SIMULATION

REFERENCES

1. R. B. Trueblood, "Advanced Flight Control System Concepts for VTOL Aircraft", MIT Instrumentation Laboratory Report R-428, 1964.

2. Military Specification, Structural Design Requirements, Helicopters (MIL-S-8698), July, 1954.

3. "The Operation of Helicopters from Small Ships", a symposium held in the Naval Air Department, Royal Aircraft Establishment, Bedford, England on 27 July 1964.

4. Stutz, R. G., Notes on Studies of VTOL and V/STOL Aircraft, a publication of Sikorsky Aircraft, June 1963.

5. Naval Warfare Analysis Group, Office of the Chief of Naval Operations, Study No. 20, The Effect of Ship Length, Ship Motions and Landing Geometry Upon the Saftey of Carrier Operations, October 1961.

6. Institute of Naval Studies, Center for Naval Analyses, The Franklin Institute, Annex D, INS Study 8, "The Influence of Ship Motion on VTOL Carrier Operations", June 1964.

7. Military Specification, Radar Set AN/APN-117 (MIL-R-21079), October 1957.

8. All Weather Flight Manual, NAVAER 00-80T-60, Rev. ed. 1961.

9. P. W. Kruse, L. D. McGlauchlin, And R. B. McQuistan, Elements of Infra-red Technology, John Wiley and Sons, Inc. New York, 1962.

10. M. R. Holter, S. Nudelman, G. H. Suits, W. L. Wolfe, and G. J. Zissis, Fundamentals of Infra-red Technology, The Mac-Millan Co., New York 1962.